Solution self-assembly of fluorinated polymers, an overview

Marc Guerre, Gérald Lopez, Bruno Améduri, M. Semsarilar, Vincent Ladmiral

REVIEW

Solution self-assembly of fluorinated polymers, an overview

Marc Guerre,[a*] Gérald Lopez,[b] Bruno Améduri,[b] Mona Semsarilar,[c] Vincent Ladmiral[b*]

Received 00th January 20xx,
Accepted 00th January 20xx

DOI: 10.1039/x0xx00000x

Abstract: Fluoropolymers constitute an attractive family of polymeric materials with remarkable properties such as high resistance to chemicals and heat, ferroelectricity and piezoelectricity for semi-crystalline polymers, to name a few. The incorporation of fluorinated blocks in a block copolymer can confer unique properties. Preparing fluorinated nanostructures through self-assembly would find use in advanced applications. Thanks to the advances made in organic and polymer chemistry, a large diversity of fluorinated monomers and polymers are available and could be used to design fluorinated copolymer architectures. This review summarizes the research performed on synthesis and solution self-assembly of fluorinated copolymers.

1. Introduction

Recent years have witnessed a continuous increase of interest in the development of nanoscale technologies dedicated to the production and control of the self-assembly of nano-objects into organized patterns.[1–5] The self-assembly of block copolymers, was particularly investigated through solution-based processes, which under particular conditions, can form sophisticated morphologies[6–9] such as spheres, cylinders, bilayer sheets and vesicles (polymersomes), to name a few. The morphologies of the self-assembled structures depend mainly on the molecular and structural characteristics of the polymer building blocks, such as composition, number of segments, segment lengths, block sequence, interactions between the blocks, interactions of the blocks with the solvent, and architecture.[10,11] The self-assembled morphologies are also substantially affected by the solution self-assembly conditions (assembly methods, solvent mixtures), external stimuli (e.g. pH, ionic strength, temperature, light irradiation…), or other polymer characteristics such as crystallinity, donor-acceptor interactions, H-bonds…).[12–15] However, the resulting assemblies are often kinetically trapped because of the inability of the system to reach the thermodynamic equilibrium. This implies that one polymer can potentially produce various (meta)stable morphologies of various topological complexities depending on the path taken toward the self-assembly.[16,17] The introduction of fluorinated segments in block copolymers endows the final self-assembled morphologies with additional properties and also often significantly modifies the self-assembly process due to the peculiar behaviour of fluorinated groups.[18] This exotic family of copolymers possesses original self-assembly behaviour due to their incompatibility with nonfluorinated segments which promotes a strong phase segregation.[19] As a result, the behaviour of amphiphilic fluorinated block copolymers remains difficult to explain due to the tendency of the fluorine-rich segments to segregate from both the hydrophilic and lipophilic segments which then result in a plethora of possible morphologies.[10,20,21] In addition, the description of these self-assembly behaviours is still largely phenomenological..

This review presents a comprehensive overview of the advances made in the synthesis and self-assembly of fluorinated block copolymers. In the first section, the common self-assembly methods are briefly described and is referred to often in the other sections of the review. This methods section is then followed by 6 chapters dedicated to different classes of fluorinated monomers and polymers ((meth)acrylates, styrenic, etc.). These chapters present and discuss the most relevant articles published to date. A special attention has been paid to multicompartment micelles, stimuli responsive nano-objects and polymerization-induced self-assembly because of the particular interest of the community for these objects and/or polymerization technique as well as the promising applications they could offer.

Self-assembly methods

Method 1: The block copolymer is gradually added into a specific solvent to one of the blocks under vigorous stirring.

[a] Laboratoire des IMRCP, Université de Toulouse, CNRS UMR 5623, Université Paul Sabatier, 118 route de Narbonne, 31062 Toulouse Cedex 9, France.
[b] ICGM, Univ Montpellier-CNRS- ENSCM Montpellier, France.
IEM, Univ Montpellier-CNRS-ENSCM, Montpellier, France.
E-mail: querre@chimie.ups-tlse.fr, vincent.ladmiral@enscm.fr
† Footnotes relating to the title and/or authors should appear here.
Electronic Supplementary Information (ESI) available: [details of any supplementary information available should be included here]. See DOI: 10.1039/x0xx00000x

Method 2: The block copolymer is dissolved in a good solvent then added to a selective solvent for one of the blocks of the polymer under vigorous stirring.
Method 3: Addition of a block copolymer solution in a good solvent to a selective solvent and removal of the good solvent by evaporation (under vacuum or not).
Method 4: Addition of a block copolymer solution in a good solvent to a selective solvent and removal of the good solvent by dialysis.
Method 5: Addition of a selective solvent to a block copolymer solution in a good solvent and removal of the good solvent by evaporation or distillation.
Method 6: Addition of a selective solvent to a block copolymer solution in a good solvent and removal of the good solvent by dialysis.
Method 7: Dialysis of a solution of the block copolymer in a good solvent against a selective solvent.

2. Poly(fluorinated(meth)acrylate)-based copolymers

2.1. Conventional self-assembly

Poly(fluorinated (meth)acrylate) copolymers possess unique properties such as low surface energies, low friction coefficients, and high insolubility in conventional solvents.[22,23] Thanks to the advent of reversible-deactivation radical polymerization (RDRP) techniques, a large number of well-defined block copolymers (BCPs) based on fluorinated (meth)acrylates have been synthesized. However, the self-assemblies of poly(fluorinated (meth)acrylate)-based BCPs have been relatively understudied compared to their fully hydrogenated counterparts. At the beginning of the century, fluorinated block copolymers and especially triphilic copolymers (amphiphilic copolymers being composed of a hydrophilic segment and two hydrophobic yet mutually incompatible segments thus generating local microphase-separation) attracted much interest. These BCPs possess the exceptional ability to form multicompartment micelles with hydrophobic, fluorophilic and hydrophilic separated domains.[21] These unusual morphologies, which favour the independent uptake and release of different (and potentially incompatible) compounds, are thought to be promising for drug delivery and controlled release strategies.[24–26]
This section dealing with the self-assembly of fluorinated (meth)acrylates-based block and hyperbranched copolymers is classified by families of fluorinated (meth)acrylates with increasing number of fluorine atoms (Scheme 1). One should bear in mind that poly(fluorinated (meth)acrylates) can be amorphous or crystalline depending on the length of their fluoroalkyl side chains. This characteristic can impact the structure of the self-assemblies (e.g. polyfluoroalkyl acrylates bearing perfluorinated side chains longer than 6 carbons are usually liquid crystalline (LC) and very hydrophobic). The use of LC properties of fluorinated copolymers is specifically addressed in the sections dealing with side chain bearing at least C_8F_{17} units or more due to their outstanding ability to form rigid and well-defined cylindrical micelles via Crystallization-Driven Self-Assembly (CDSA).

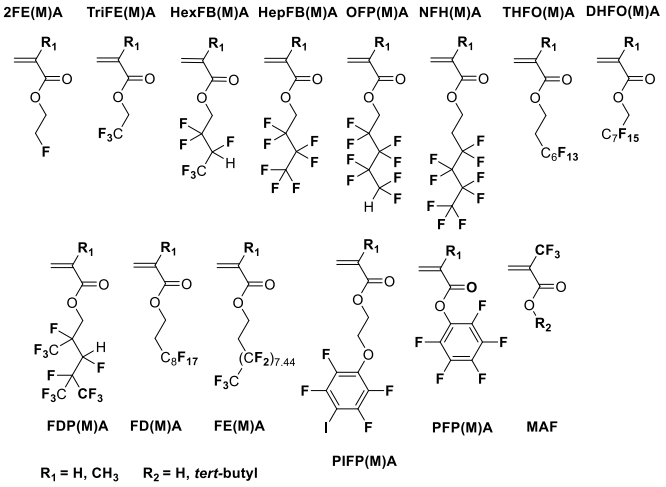

Scheme 1. Structures of the referred self-assembled fluorinated (meth)acrylates copolymers. 2-Fluoroethyl (meth)acrylate (2FE(M)A), 2,2,2-Trifluoroethyl (meth)acrylate (TriFE(M)A), 2,2,3,4,4,4-Hexafluorobutyl (meth)acrylate (HexFB(M)A), 2,2,3,3,4,4,4-Heptafluorobutyl (meth)acrylate (HepFB(M)A), 2,2,3,3,4,4,5,5-Octafluoropentyl (meth)acrylate (OFP(M)A), 3,3,4,4,5,5,6,6,6-Nonafluorohexyl methacrylate (NFHMA), 1H,1H,2H,2H-Perfluorooctyl methacrylate (THFOMA), 1H,1H-Perfluorooctyl methacrylate (DHFOMA), Dodecafluoroheptyl methacrylate (FDPMA), 1H,1H,2H,2H-Perfluorodecyl (meth)acrylate (FD(M)A), Perfluoroalkyl ethyl methylacrylate (FEMA), Iodotetrafluorophenoxy methacrylate (IFPMA), pentafluorophenyl methacrylates (PFP(M)A), 2-(Trifluoromethyl)acrylic acid and its ester (MAF).

2.1.1. *2*-Fluoroethyl (meth)acrylate (2FE(M)A)

In 2011, He et al. reported the self-assembly of linear triblock terpolymers consisting of P*n*BMA-*b*-PMMA-*b*-P2FEMA (PnBMA= poly(n-butyl methacrylate and PMMA = poly(methyl methacrylate)) synthesized by sequential RAFT (Reversible Addition-Fragmentation chain Transfer) polymerization.[27] The copolymers were self-assembled using method 2 in a mixture of THF (good solvent) and methanol (bad solvent) and led to well-defined and uniform spherical aggregates. The lack of other articles dealing with the self-assembly of 2FE(M)A-containing BCP likely lies in the minor influence of the fluorinated atom over the final morphologies.

2.1.2. *2,2,2*-Trifluoroethyl (meth)acrylate (TriFE(M)A) Block Copolymers

In 2012, the Whittaker's group reported the effect of the solvent on the self-assembly behaviour of PAA-*b*-P(*n*BA-*co*-TriFEA) (AA= acrylic acid)copolymers prepared by sequential Atom Transfer Radical Polymerization (ATRP).[28] The triblock copolymers were initially dissolved in acetone or DMF and analysed by Transmission Electron Microscopy (TEM). At that point, the copolymer solutions were dialyzed against deionized water and characterized by TEM. In pure DMF, large aggregates were observed, while in acetone, cylindrical structures were formed, consistent with predictions based on the relative polymer-solvent interaction parameters. Upon addition of water, both systems formed cylindrical micelles. The same group also reported multifunctional hyperbranched

copolymers containing iodine and fluorine atoms for applications as Magnetic Resonance Imaging (MRI) contrast agents and bimodal imaging agents.[29]

Later, in 2014 Li et al. reported the self-assembly of PMMA-*b*-PTriFEMA diblock copolymer synthesized by RAFT polymerization. The self-assembled morphologies were relatively ill-defined with the formation of large aggregates (> µm) due to the use of water as the structuring solvent (bad solvent for both blocks).[30] The same year, Muraro et al. reported the synthesis of POEGMA–*b*-PTriFEA (OEGMA = oligoethylene glycol methacrylate) block copolymers by RAFT.[31] These copolymers formed well-defined sub-100 nm spherical particles using methods 1 and 6. In view of developing stimuli-responsive aggregates, Zhang and Zhu prepared CO_2- and O_2-responsive polymer vesicles consisting of an hydrophilic polyethylene glycol (PEG) block, a CO_2-responsive PDEAEMA (poly(2-diethylamino)ethylmethacrylate)) block and an O_2-responsive PTriFEMA block copolymers.[32]

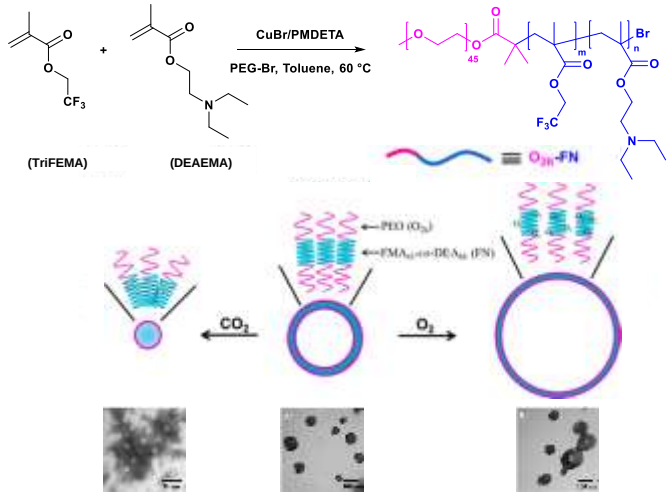

Fig. 1 Synthetic routes of CO_2- and O_2-sensitive block copolymers. Schematic representations and TEM pictures of CO_2- and O_2-driven self-assemblies in water of PEG-*b*-PDEAEMA-*b*-TriFEMA triblock copolymers. Adapted with the permission from ref. [32]. Copyright 2014 ACS.

The PEG-*b*-PDEAEMA-*b*-TriFEMA triblock copolymer was synthesized by ATRP in 2 steps from PEG macro-CTA (CTA = chain-transfer agent) and self-assembled in water into vesicular nanoaggregates using method 4. When treated with CO_2, the vesicular morphology transformed into objects of smaller size, to accommodate the increased interfacial free energy. When treated with O_2, the vesicular morphology was preserved, but its volume expanded (Fig. 1). This phenomenon was attributed to the intermolecular interaction between O_2 and PTriFEMA that slightly increased the water solubility of the fluorinated hydrophobic block.

gradient, graft, hyperbranched copolymers)

In addition to block copolymers architectures, other architectures such as gradient or graft copolymers were also studied. Chen et al. reported the self-assembly in different solvent mixtures of PAA-*grad*-PTriFEMA gradient copolymers prepared by RAFT.[33] Although the authors claimed that the copolymers self-assembled in selective solvents to form crew-cut micelles with different ordered structures and a certain degree of tunability depending on the solvent, their conclusions may be surmised considering the TEM images provided. Graft copolymers were reported by Xu et al. who studied the self-assembly of bottlebrush polymers composed of PTriFEMA side chains and polynorbornene backbones, synthesized *via* ATRP and Ring Opening Metathesis Polymerization (ROMP).[34] A PNB-*g*-PTriFEMA graft copolymer was self-assembled using method 1 and formed near-spherical particles with a diameter of ca. 10 nm, corresponding to the dimensions of a single chain. When the L/D ratio was gradually increased (with L standing for the backbone length and D the side chain length), the self-assembled microstructures evolved nicely and transitioned from elongated shapes toward "spherical" particles with a diameter of *ca.* 25 nm suggesting partial coiling of the backbone. Wooley and coworkers[35] synthesized hyperbranched-star amphiphilic TriFEMA-based fluorinated polymers with a core-shell morphology. These amphiphilic fluorinated hyperbranched-star polymers were then self-assembled into 20 nm polymer micelles, which presented attractive properties for applications in ^{19}F MRI.

2.1.3. *2,2,3,4,4,4*-Hexafluorobutyl (meth)acrylate (HexFB(M)A)

Block copolymers

Diblock copolymers[36] containing HexFBMA have been much less studied compared to triblock copolymers. In 2014, Feng and co-workers[37] pioneered the synthesis and self-assembly of CO_2-switchable multi-compartment micelles (MCMs) prepared from a linear ABC triblock copolymer synthesized by RAFT polymerization. The ABC block copolymer was composed of a PHexFBMA block, a hydrophilic polyethylene oxide (PEO) block, and a CO_2-responsive block of PDEAEMA. The triblock copolymer was self-assembled using method 7. In the first place, the micelles appeared as spherical with only little phase segregation in the core (Fig. 2a). However, after treatment with CO_2, the aggregates showed clear segregated microdomains typical of MCMs with various phase-segregated morphologies such as "hamburgers" (1, Fig. 2b), "reverse hamburgers" (2, Fig. 2b), "clovers" (3, Fig. 2b), "soccer ball" (4, Fig. 2b) and more complicated structures (5, Fig. 2b). Interestingly, these morphological transitions were completely reversible and could be switched "on" and "off" by treatment with CO_2 and N_2 via simple protonation and deprotonation of the tertiary amine groups.

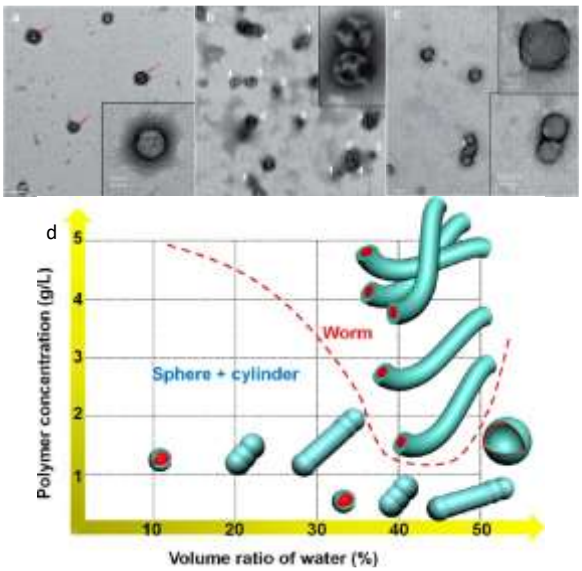

Fig. 2. a-c) TEM images of PEG-*b*-PHexFBMA-*b*-PDEAEMA triblock copolymer self-assemblies in water. (a) before bubbling CO_2, (b) after bubbling CO_2, and (c) after CO_2 removal by N_2 bubbling. Reproduced with the permission from ref. [37]. Copyright 2014 RSC. d) Phase diagram of the PEG-*b*-PHexFBMA-*b*-PDEAEMA triblock copolymer in water/ethanol mixed solvent as a function of volume ratio of water and polymer concentration. Reproduced with the permission from ref. [38]. Copyright 2015 ACS

When they employed self-assembly method 1, worm-like micelles (WLMs) were formed.[38] Under this regime, an evolution from spherical micelles to short rods, cylinders, and finally worm-like micelles were observed when the water content of a water/ethanol binary mixture was increased from 0 to 50% (Fig. 2d). The authors also showed that higher polymer concentrations favoured the formation of WLMs, while the morphology was less affected by the length of the PDEAEMA block. The latest study of the same group reported the synthesis of a series of PEG-*b*-PHexFBMA-*b*-PDEAEMA triblock copolymer nanoparticles. The majority of the morphologies obtained were spherical particles even after exposure to CO_2. Only triblock copolymers with volume fractions of 0.34 to 0.38 of PHexFBMA, transformed from spherical micelles to multi-compartment micelles after reaction with CO_2.[39]

Graft copolymers

The graft copolymers were the second class of macromolecular architectures predominantly investigated for HexFPMA. Xiong et al. described the synthesis, self-assembly and encapsulation properties of a series of amphiphilic graft copolymers (PHexFBMA-*g*-PSPEG) synthesized by conventional free radical polymerization comprised of PHexFBMA backbone and PEG side chains (SPEG was synthesized by reacting Methoxy poly(ethylene glycol) (MPEG) with p-chloromethylstyrene in THF).[40] Self-assembly using method 1 resulted in the formation of spherical morphologies that evolved to worm- and vesicle-like structures upon addition of bovine serum albumine. Later, in 2016, Pang's group[41] reported the preparation of well-defined thermoresponsive block-graft copolymer, PHexFBMA-*b*-(PGMA-*g*-PNIPAM) using ATRP and Copper-catalyzed Azide-Alkyne Cycloaddition (CuAAC) coupling reaction (PNIPAM= poly(N-isopropyl acrylamide and (PGMA = poly (poly(glycidyl methacrylate))). The copolymers were self-assembled using method 5. TEM images showed stable spherical nanoparticles with diameters of 30–40 nm at 20 °C. Larger and more irregular particles were formed at more elevated temperatures (40-60 °C) due to the phase transition of the thermosensitive PNIPAM segments.

2.1.4. *2,2,3,3,4,4,4*-Heptafluorobutyl (meth)acrylate (HepFB(M)A)

In 2011, Laschewsky's team reported original morphologies from self-assembly of amphiphilic triblock copolymers composed of hydrophilic poly(oligoethylene glycol acrylate) (POEGA), lipophilic PBzA (poly(benzyl acrylate), and fluorophilic HepFBA, synthesized by sequential RAFT polymerizations.[42] The self-assembly was performed in water using method 5. The resulting morphologies obtained after annealing, were unique with segregated domains forming structures resembling "soccer ball" (Fig 3a) or bi-spherical/acorn micelles (Fig 3b). Studies on different copolymer compositions, revealed that the morphologies depended on the length of the individual blocks as well as the block sequence. Quite uniquely, it was demonstrated that the fluorinated and hydrocarbon low molar mass compounds could be solubilized selectively in the respective fluorophilic and lipophilic domains.

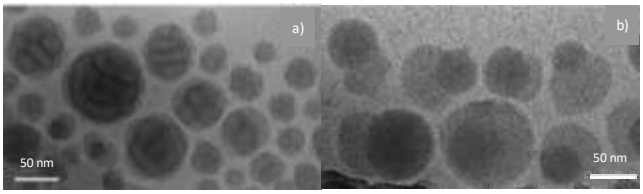

Fig 3. a) "Soccer ball" morphologies observed by cryo-TEM images of a 0.5 wt.% solution of $PBzA_{45}$-*b*-$POEGA_{40}$-*b*-$PHepFBA_{30}$ in water after annealing for 2 weeks at 75 °C. b) Bi-spherical morphologies observed by cryo-TEM images of a 0.5 wt.% solution of $PBzA_{45}$-*b*-$POEGA_{175}$-*b*-$PHepFBA_{40}$ in water after annealing for 2 weeks at 75 °C. Reproduced with the permission from ref. [42]. Copyright 2011 ACS.

Following this work, Zhou et al. reported the synthesis and self-assembly of PS-*b*-PHepFBMA (PS= polystyrene) diblock copolymers synthesized by sequential ATRP.[43] The diblock copolymers were self-assembled in THF/EtOAc binary mixture using method 2. The authors showed that the assemblies evolved from spheres to vesicles with increasing content of EtOAc in the solvent mixture. In 2015, Singha and co-workers reported the RAFT synthesis of PPEGMA-*b*-PHepFBA diblock copolymer and their self-assembly in water using method 1 that resulted in formation spherical micelles.[44] This diblock copolymer was also successfully used as a surfactant and macro-RAFT agent (surf-RAFT agent) for the mini-emulsion polymerization of styrene. The same authors also reported the synthesis and self-assembly of PMMA-*b*-PHepFBA diblock copolymers.[45] These diblock copolymers were self-assembled via method 2 in Methyl Ethyl Ketone: Tetrahydrofuran (MEK:THF) binary mixtures. The self-assembled morphologies, depending on the THF:MEK volume ratios, were claimed to be micelles, worms and nanotubes, although the evidence provided may not be sufficiently convincing. In a different approach, Luo and co-workers employed (PDMS-*b*-PMMA-*b*-PHepFBMA, a silicone-containing triblock copolymers,) to

stabilize gold nanoparticles (PDMS = poly (dimethyl siloxane).[46] They also reported the self-assembly of amphiphilic gradient copolymer poly(AA-*grad*-HepFBMA) in THF/ H_2O mixtures (16≤ H_2O (%) ≤84) forming mainly ill-defined morphologies, containing few unusual morphologies such as cubic or circles.[47]

2.1.5. *2,2,3,3,4,4,5,5*-Octafluoropentyl (meth)acrylate (OFP(M)A)

The group of P. Ni was the first to study the self-assembly of POFPMA-containing copolymers. In 2007, they pioneered the synthesis (via oxyanion-initiated polymerization)[48] and self-assembly of fluorinated hyperbranched star-block copolymers composed of hyperbranched poly[3-ethyl-3-(hydroxymethyl)oxetane] cores, and PDMAEMA (poly((2-dimethylamino)ethyl methacrylate)) and POFPMA as the arms.[49] Using method 1 in acidic aqueous solution, the copolymers self-organized into multicompartment micelles. When DMF:water binary mixture was used, the copolymer with short PDMAEMA segment, self-assembled into well-dispersed multicompartment micelles, while copolymer with twice as long PDMAEMA formed nanofibers/thread-like morphologies. The same team later worked on more defined block copolymers architectures.[50] Using the same synthetic procedure, they synthesized POFPMA-*b*-PEO-*b*-PPO-*b*-PEO-*b*-POFPMA, (PPO = polypropylene oxide) an amphiphilic pentablock copolymers. Self-assembly using method 1 led to the formation of well-defined frozen micelles while method 3 resulted in more complex morphologies such as multicompartment micelles or vesicles depending on the length of the fluorinated block. They also investigated the self-assembly of double-hydrophilic, fluorinated monomethyl end-capped poly(ethylene glycol)-*b*-poly[2-(dimethylamino)ethyl methacrylate]-*b*-poly(2, 2, 3, 3, 4, 4, 5, 5-octafluoropentyl methacrylate) (MePEG-*b*-PDMAEMA-*b*-POFPMA) triblock copolymer, synthesized via oxyanion-initiated polymerization.[51] These triblock copolymers were self-assembled using method 1 in water at pH 7. Spherical morphologies were mainly observed, but a transition from sphere to rod morphologies when the lengths of the MePEG and PDMAEMA blocks were reduced. In another report, they elegantly studied and compared the self-assembly behaviour of PIB-*b*-PDMAEMA-*b*-POFPMA (PIB = polyisobutylene) and PS-*b*-PDMAEMA-*b*-POFPMA triblock copolymers using method 1.[52] This study demonstrated that the flexible PIB block strongly influenced the nature of the self-assembled morphologies, which evolved from spherical multicompartment micelles to fiber-like aggregates, nanotubules, and finally rod-like aggregates upon increasing the polymer concentration (Fig 4, left). Conversely, the rigid PS-based system self-assembled into multicompartment micelles, hamburger-like structures and flowerlike nanoparticles (Fig 4, right). Zhuang's group reported in two complementary studies the self-assembly behaviour of miktoarm POFPMA-based block copolymers prepared by ATRP and CuAAC coupling.[53,54] Method 4 was used for the self-assembly which resulted in the formation of spherical particles. Block copolymers with longer POFPMA block, formed an array of nanostructures, ranging from simple and patchy spherical micelles and aggregates to vesicles.

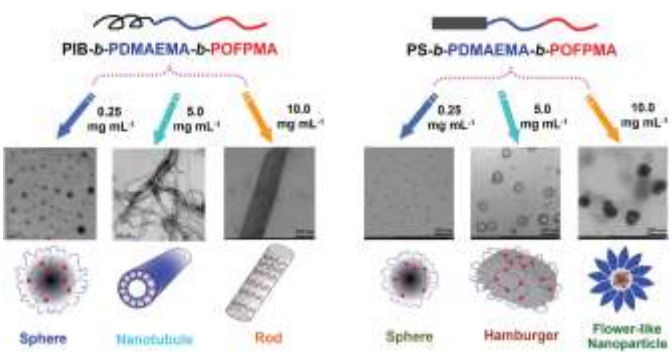

Fig 4. Schematic illustration and TEM images of the numerous hierarchical assemblies formed from PIB-*b*-PDMAEMA-*b*-POFPMA and PS-*b*-PDMAEMA-*b*-POFPMA triblock terpolymers. Reproduced with the permission from ref. [52]. Copyright 2016 RSC.

Other morphologies were also observed such as raspberry-like, concave patchy, brush-like, segmented worm-like micelles and perforated stomatocytes. Similar triblock copolymers based on PEG, PLA (poly (lactic acid)) and POFPMA were also reported with potential application as ultrasound contrast agent.[55]

2.1.6. *3,3,4,4,5,5,6,6,6*-Nonafluorohexyl methacrylate (NFHMA)

NFHMA-based copolymers and their self-assembly are scarce in the literature. In 2004, Matsuoka's group reported for the first time the synthesis and self-assembly of well-defined PNaMA-*b*-PNFHMA (NaMA = sodium methacrylate) amphiphilic diblock copolymers synthesized by anionic polymerization.[56] Using method 1, these block copolymers formed micelles in aqueous solution. Dynamic Light Scattering (DLS), Small Angle X-ray Scattering (SAXS) and Small Angle Neutron Scattering (SANS) analyses revealed that these diblock copolymers formed larger micelles than their nonfluorinated analogs. The authors also demonstrated the fluorophilicity of PNaMA-*b*-PNFHMA diblock copolymers by selective solubilization of fluorinated low molar mass compounds (decafluorobiphenyl and 2,6-dimethylnaphthalene). Later, Wang et al. described the aqueous self-assembly (method 3) of MePEG-*b*-PCL-*g*-PNFHMA terpolymers synthesized by Ring Opening Polymerization (ROP) and ATRP (PCL = poly(ε-caprolactone).[57] Because of the incompatibility of PCL and PNFHMA, well-segregated Janus-cores were formed. These findings demonstrated once again that the architecture of each hydrophobic segment can play a significant role in the formation of specific compartmentalized structures.

2.1.7. *1H,1H,2H,2H*-Perfluorooctyl methacrylate (THFOMA)

In 2003, Hussain et al. described the self-association properties of di- and ABA triblock copolymers synthesized by ATRP, containing PEO as the hydrophilic (B) and PTHFOMA as the hydrophobic block (B).[58] The block copolymers were self-assembled in water using method 1 and were analysed by DLS and TEM. DLS revealed the existence of various types of

aggregates in solution, including single chains, micelles, and large clusters. Surprisingly, only large clusters were detected in the case of the triblock copolymers. In addition, depending on the initial concentration, single chain micelles, fibrous networks, and ill-defined aggregates were revealed by TEM. Then in 2004, Hwang et al. reported the synthesis by ATRP of diblock and statistical copolymers from OEGMA and THFOMA and their self-assembly using method 1 in water and chloroform.[59] In water, spherical micelles were formed, while in chloroform, a mixture of worm-like micelles and large aggregates were observed, depending on the blocks lengths. In 2016, Sawamoto reported multipode self-folding copolymers obtained from thermoresponsive intramolecular self-assembly of PEG–methacrylate and THFOMA random copolymers in water, DMF, and 2H,3H-perfluoropentane (2HPFP).[60] The random copolymers were efficiently prepared by ruthenium-catalysed living radical copolymerization. They displayed various self-folding structures and local associations. The authors also showed that replacing the poly(ethylene glycol) by trehalose caused increased the polarity difference with the fluorinated hydrophobic segment and changed the aggregation state of the polymer in water. The PEG-fluorinated and trehalose/PEG-fluorinated amphiphilic random copolymers were the most efficient at encapsulating novaluron, a fluorinated agrochemical. The presence of the agrochemical exerted a substantial influence on the self-assembly of the polymers, demonstrating that fluorous interactions altered the intramolecular self-folding behaviour and intermolecular polymer association which lead to the formation of well-defined nanoparticles.[61] In addition, they designed **A/C–B/C** random block copolymers, introducing hydrophobic dodecyl ($-C_{12}H_{25}$, **A**) and hexafluorooctyl pendant groups ($-C_2H_4C_6F_{13}$, **B**) into the blocks, and hydrophilic poly(ethylene glycol) pendant groups (PEG, **C**) randomly placed into both blocks. By controlling the DP and the composition of this block copolymer, the self-assembly led to the formation of double core, tadpole and multi-compartment micelles in water.[62]

2.1.8. *1H,1H*-Perfluorooctyl methacrylate (DHFOMA)

The synthesis and self-assembly of DHFOMA copolymers have exclusively been reported by Lee et al.[63] They synthesized block copolymers of hydrophilic PEO and hydrophobic PDHFOMA by ATRP of PDHFOMA from a PEO-macro-initiator. The direct dissolution of the block copolymer in chloroform (method 1) resulted in the formation of well-ordered spherical particles with average diameter of 12-26 nm.

2.1.9. Dodecafluoroheptyl methacrylate (FDPMA)

Xu and Liu examined PAA-*b*-PFDPMA diblock copolymers for the first time.[64] Synthesized by RAFT, these amphiphilic block copolymers were self-assembled using method 6 with 2-butanone as the good solvent and water:methanol binary mixtures as the selective solvent (2-butanone and methanol were removed by dialysis). TEM revealed various morphologies: spheres, rods, and vesicles depending on the initial water fraction in the water/methanol binary mixtures. Addition of fluorinated hydrophobic homopolymers converted the spheres, rods, and vesicles into large spheres. Dong et al. studied the self-assembly of PMMA-*b*-PFDPMA diblock copolymers synthesized by ATRP.[65] These diblock copolymers were self-assembled using method 1 in chloroform, THF and trifluorotoluene (TFT). In chloroform, comb-shape particles were observed (Fig. 5a) (. In THF, spherical particles were formed with dark fluorinated centres and lighter hydrogenated edges (Fig. 5b). In TFT, the aggregates were simply constituted of homogeneous unimers due to the good solubility of both PMMA and PFDPMA in the solvent (Fig. 5c). Multiblock copolymers were also investigated by Tuo et al., who synthesized tetraphenylethane-based polyurethane (PUMI) as macroiniferter for the conventional radical polymerization of FDPMA. This polymer self-assembled into various nanostructures in the course of the polymerization.[66] The incompatibility of FDPMA and PUMI lead to significant decrease of the solubility of PUMI in DMF with the addition of FDPMA monomer, and drove the formation of multicore particles. These morphologies evolved into arrays of disk-like structures, while the smallest particles formed nanofibers.

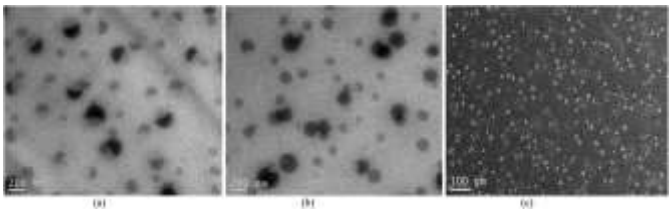

Fig. 5. TEM pictures of PMMA-b-PFDPMA diblock copolymers in CHCl3 (a), THF (b), and TFT (c) solutions. Light area = PMMA, dark areas = PFDPMA. Reproduced with the permission from ref. [65]. Copyright 2012 RSC

Pan et al. reported the synthesis and self-assembly of linear POSS–PMMA-*b*-PFDPMA (POSS = Polyhedral Oligomeric Silsesquioxane) and star-shaped (s-POSS–PMMA-*b*-PFDPMA) diblock copolymers.[67] Self-assemblies were achieved in THF using method 1 and led to the formation of core/shell micelles. In another study, the same group synthesized 1/2/4/6-arm architectures of PMMA-*b*-POSS-*b*-PFDPMA. All four structures self-assembled into spherical core-shell micelles (100-250 nm) in THF. The size of the micelles was inversely related to the number of arms (smaller aggregates with increasing number of arms)[68]

2.1.10. 1H,1H,2H,2H-Perfluorodecyl (meth)acrylate (FD(M)A)

FDMA-based copolymers are by far to the most studied acrylic-based fluorinated polymers. This is due to its high fluorophilicity that could lead to unusual morphologies as well as its tendency to form crystalline cylindrical micelles due to the presence of C_8F_{17} side chains and their liquid crystalline property. The first self-assembly of FD(M)A-based copolymers was reported in 2000 by Imae et al. who investigated the self-assembly of PMMA-*b*-PFDMA and P*t*BMA-*b*-PFDMA (*t*BMA = *tert*-butyl methacrylate) diblock copolymers in acetonitrile and chloroform.[69] Spherical aggregates were observed by cryo-TEM in both solvents. Furthermore, the authors investigated the influence of NaCl which induced electrostatic repulsions in the

poly (methacrylic acid) (PMAA) chains resulting in the formation of small micelles. Later, the Laschewsky's group reported the RAFT polymerization of butyl acrylate or 2-ethylhexyl acrylate (EHA), and FDMA using a PEO macromolecular chain transfer agent. The resulting linear amphiphilic diblock and triblock copolymers were self-assembled using method 5 at room temperature and at 70 °C.[70] In both cases, the polymers formed stable micellar aggregates for a prolonged period of time. However, fluorinated nano-domains in the micelle cores were not observed possibly because of their size.[70] Later, the same authors reported the synthesis and aqueous self-assembly of PEHA-*b*-POEGA-*b*-PFDA triblock copolymer using method 5.[71] In contrast to their previous study, this triblock copolymer self-assembled into unusual "soccer ball-like" multicompartment micelles due to the incompatibility of the POEGA and PFDA hydrophobic blocks (Fig. 6). In 2010, they explored the self-assembly of a series of POEGA-*b*-PFDA, POEGA-*b*-PBA-*b*-PFDA and PEHA-*b*-POEGA-*b*-PFDA block copolymers.[72] The block copolymers were self-assembled in water using methods 3 and 6. Whereas only spherical aggregates without phase segregation were observed for the POEGA-*b*-PFDA diblock copolymer, unprecedented multicompartment morphologies, such as "patchy double micelle" and larger "soccer ball" structures were identified for POEGA-*b*-PBA-*b*-PFDA and PEHA-*b*-POEGA-*b*-PFDA triblock copolymers.[72]

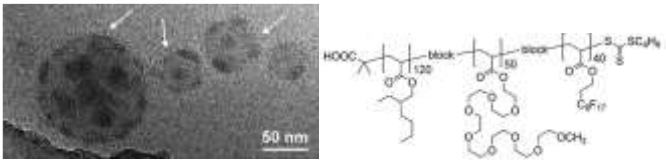

Fig. 6. Cryo-TEM micrographs of PEHA-*b*-POEGA-*b*-FDA triblock copolymer self-assembled in water. Reproduced with the permission from ref. [71]. Copyright RSC 2009.

The concept was further investigated by Gao et al. on PAA-*b*-PCOEMA-*b*-PFDMA or PtBA-*b*-PCOEMA-*b*-PFDMA (PCOEMA = poly(2-cinnamoyloxyethyl methacrylate) triblock copolymers.[73] Using method 1, almost all triblock copolymers generated cylindrical micelles at room temperature in different TFT/alcohol binary mixtures. The sole exception was the triblock copolymer with the lowest PFDMA mass fraction and the highest soluble block mass fraction which formed a mixture of cylindrical and spherical micelles. All the micelles possessed a PFDMA core, a PCOEMA shell, and a PAA or PtBA corona. TEM images indicated that the PFDMA chains in the core were almost fully stretched and that the PCOEMA chains in the PAA/PCOEMA/PFDMA cylindrical micelles were radially compressed. More exotic morphologies and shapes resembling triangles, rhombus, squares as well as ring, eye- and racket-shaped aggregates were also reported later by the same authors on similar BCPs.[74] The authors suggested that the formation of cylindrical morphologies was driven by the fluorinated-block yielding cylinders with abnormal shell thicknesses. The singular LC property of PFDMA copolymers was used again by Manners and co-workers in P2VP-*b*-PFDMA (P2VP = poly(2-vinylpyridine) LC diblock copolymers prepared by sequential anionic polymerization.[75] In a first attempt, using method 1, cylindrical micelles governed by the crystallinity of the fluorinated block were obtained with relative broad length distribution. Yet, using a fragmentation *via* sonication followed by annealing, the authors were able to produce monodisperse cylindrical micelles with controlled lengths. The broad length distribution likely caused by the low energy barrier of nucleation and fast growth process, was later addressed by addition of small molecules to the solution of similar block copolymers (see Fig. 7) inducing supramolecular interactions.[76] These interactions resulted in the formation of hierarchical nanostructures with precise control over their size via a three-step assembling strategy (Fig. 7). The observed morphologies were linear, branched, segmented, hairy plate-like, and star-like nanostructures.

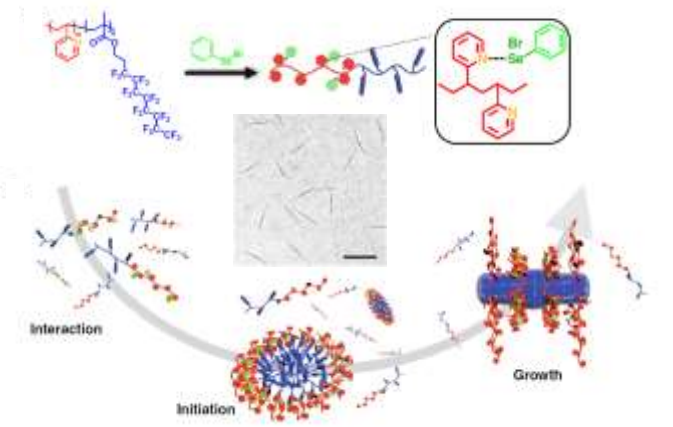

Fig. 7. Chemical structures and schematic representation of the P2VP-*b*-PFDMA block copolymers with detailed cylindrical driven growing 3-step process. Interaction: PhSeBr initiators form complexes with the pyridyl groups. Initiation: these interactions result in less soluble complex which tends to aggregate enabling to PFMA chains a higher propensity to form oligomeric aggregates with LC cores. Growth: formed complexed aggregates served as seeds for the growth of the free monomeric polymer chains driven by the LC ordering effect. Adapted with the permission from ref. [76]. Copyright Springer Nature 2019.

2.1.11. Perfluoroalkyl ethyl methylacrylate (FEMA)

To date only one article reports the self-assembly of PFEMA-based copolymers. Li et al. prepared P(MMA-*co*-MAA)-*b*-PFEMA diblock copolymers by RAFT polymerization and self-assembled them in water using method 3.[77] The triphilic copolymers (hydrophilic, lipophilic, and fluorophilic due to MAA, MMA, and FEMA, respectively) displayed nanostructures, such as spheres and short worms that evolved to worms, tapered worms, and finally to nail-shaped structures, as the water content increased from 10, to 80 vol. %. This morphological transition upon addition of water was ascribed to the increase of the interfacial tension between the core-forming block and the solvent.

2.1.12. Iodotetrafluorophenoxy methacrylate (IFPMA)

This peculiar iodine atom-bearing fluorinated monomer was investigated to examine the effect of halogen-interactions[78] in the formation of hierarchical morphologies. Taylor et al. described an attractive method based on non-covalent halogen bonding interactions as the driving force for the solution self-assembly of fluorinated copolymers.[79] First, a PEG-*b*-PDMAEMA

diblock copolymer was synthesized by ATRP as the halogen-bond acceptor, then PEG-*b*-PIFPMA diblock copolymer was prepared by RAFT as the halogen-bond donor. Mixing the donor and the acceptor, resulted in the formation of higher-order structures in organic solvents as well as in water.

2.1.13. 2-(Trifluoromethyl)acrylic acid and its ester (MAF)

2-(Trifluoromethyl)acrylic acid (or MAF) and its esters do not homopolymerize via radical polymerization. They however readily copolymerize with more electron-rich olefins such as vinyl acetate for example.[80–82] Falireas et al.[83] recently prepared amphiphilic diblock terpolymers composed of a PNIPAM or PDMA (DMA = *N*, *N*,-dimethyl acrylamide) hydrophilic block and an hydrophobic poly(MAF-TBE-*alt* VAc) block (MAFTBE = *tert*-butyl-2-trifluoromethacrylate) via sequential RAFT polymerization. Hydrolysis of the ester groups produced double hydrophilic diblock terpolymers endowed with pH-responsiveness (and also thermoresponsiveness for the PNIPAM-based BCP). Both the hydrolysed and the non-hydrolyzed BCP were shown to form vesicular structures by self-assembly.

2.1.14. Mixture of monomers

In addition to copolymers containing a single fluorinated monomer family, other copolymers composed of different fluorinated moieties were also investigated, leading to simple micelles or less well-defined morphologies. For instance, Hwang et al. reported the preparation of amphiphilic semifluorinated block copolymers composed of PDMAEMA as the hydrophilic block and PDHFOMA or PTHFOMA block as the fluorinated block.[84] The size of the micelles were shown to be influenced by the copolymer composition, the pH, and the temperature. Niu et al. also reported the self-assembly of complex multiblock architectures consisting of a fluorosilicone block extended with PMMA and polymers of various fluorinated methacrylates such as TriFEMA, HexFBMA, OFPMA, and FDMA.[85] The self-assembly behavior were difficult to predict and led to pure micelles or unimers depending on the solvent used. Mugemana et al. studied a number of fluorinated amphiphilic star block-copolymers starting from tris(benzyltriazolylmethyl)amine and composed of diblocks of polypentafluorostyrene (PPFS), PHepFBA, or PTHFOA and hydrophilic p-oligo(ethylene glycol) styrene (POEGSt) or POEGMA.[86] Spherical aggregates with diameters ranging between 20 and 50 nm were the main structures observed for PFS-, HepFBA- and PTHFOA-containing copolymers. Increasing the mass fraction of PHepFBA led to the formation of unilamellar and multilamellar vesicles.

2.2. Polymerization-Induced Self-Assembly (PISA)

Polymerization-Induced Self-Assembly (PISA) has emerged as an extremely effective technique to prepare self-assembled polymer aggregates with controlled and defined morphologies at high solids contents with high reproducibility.[87–97] Under PISA process, a solvophilic polymer precursor dissolved in a solvent is extended with a solvophobic polymer. As the polymerization proceeds, the chain extension leads to the formation of an "amphiphilic" block copolymer that self-assembles into colloidally stable nano-objects. When combined with RAFT polymerization technique (the most commonly used RDRP techniques in PISA), it allows the formation of diverse morphologies such as spheres, worm-like micelles and vesicles for example. So far, most PISA protocols have used RAFT polymerization in dispersion or emulsion and involved hydrogenated acrylic monomers. However, a few articles report the use of fluorinated monomers in PISA formulation.

2.2.14. Alkyl perfluorinated (meth)acrylate

In 2008, Howdle pioneered the use of fluorinated macro-RAFT agent for the surfactant-free polymerization of MMA in $scCO_2$.[98] A PDHFOMA RAFT macro-CTA was chain extended with MMA. The polymerization exhibited excellent control under dispersion polymerization conditions and resulted in well-defined core-shell spherical particles (1-5 µm). Xu et al. revisited this study and used fluorinated methacrylate (with pendant $-C_6F_{12}H$ group) to polymerize MMA via PISA protocols in $scCO_2$.[99] Spherical nanoparticles with different size and polydispersity were obtained. Armes and coworkers reported the morphological transition of PMAA-*b*-PbzMA block copolymer nanostructures upon chain extension with TriFEMA in ethanol under dispersion polymerization conditions (Fig. 8).[100]

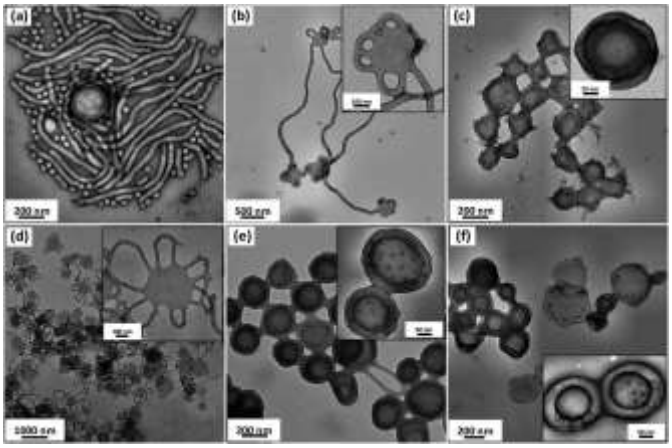

Fig. 8. Representative morphologies obtained after dispersion PISA of TriFEMA in ethanol. a) $PMAA_{70}$-*b*-$PBzMA_{100}$-*b*-$PTriFEMA_{100}$; (b) $PMAA_{70}$-*b*-$PBzMA_{200}$-*b*-$PTriFEMA_{200}$; (c) $PMAA_{70}$-*b*-$PBzMA_{70}$-*b*-$PTriFEMA_{223}$; (d) $PMAA_{70}$-*b*-$PBzMA_{191}$-*b*-$PTriFEMA_{60}$; (e) $PMAA_{70}$-*b*-$PBzMA_{243}$-*b*-$PTriFEMA_{60}$; (f) $PMAA_{70}$-*b*-$PBzMA_{273}$-*b*-$PTriFEMA_{60}$. Reproduced with the permission from ref. [100]. Copyright 2014 RSC.

The same group used the same concept with PMAA and PDMAEMA RAFT macro-CTAs that they chain-extended with TriFEMA.[101] TEM images indicated that well-defined spherical nanoparticles were produced in both cases. In contrast, a shorter PDMAEMA macro-CTA led to the formation of spheres, which evolved into worms and polydisperse vesicles depending on TriFEMA conversion. This evolution of the self-assembled morphologies was caused by the gradual reduction in the molecular curvature of the growing copolymer chains. The Armes group also performed detailed SAXS studies to

determine the effective particle density, steric stabilizer layer thickness as well as the volume-average number of a series of PGMA-*b*-PTriFEMA nanoparticles synthesized by PISA (PFMA = poly(glycerol monomethacrylate)).[102] In addition, they also prepared similar but transparent diblock copolymer nanoparticles (PSMA-*b*-PTriFEMA) in *n*-alkane at different concentrations (PSMA = poly(stearyl methacrylate)). The transparency was due to the matching refractive indexes of PTriFEMA and *n*-alkane.[103,104] Such particles find use in smart (such as anti-reflective) coatings. Similarly to the work reported by Armes and co-workers,[101] Li's group reported a PISA process using a PMAA macro-CTA and PTriFEMA as the core-forming fluorinated polymer.[105] TriFEMA was also recently used in the PISA formulation of polymer nano-objects for cell uptake and tracking *via* ^{19}F MRI.[106] Detrembleur et al. used aqueous PISA for the preparation of transparent superhydrophobic coatings.[107] Hydrophilic PMAA macro-CTA was synthesized, and chain-extended with FDMA and *n*-butyl acrylate to produce stable fluorinated particles which were successfully spin-coated with fillers to produce superhydrophobic transparent coatings after further treatment. Ma's group reported the ab initio emulsifier-free emulsion copolymerization of a mixture of monomers including HexFBMA. However, they did not provide enough evidence of the successful copolymerization of the monomer mixture or of the efficient chain extension of the PDMAEMA-*b*-PHexFBA macro-CTA.[108,109] The same group also reported the formation of stabilized spherical particles in ethanol using PAA and PHexFBMA as hydrophilic block and fluorophilic/hydrophobic block respectively.[110,111] Spherical core-shell latex particles were formed as judged by TEM and DLS studies. The size of these latex particles could be increased by increasing the pH. Huo et al. reported the seeded RAFT dispersion polymerization of THFOMA using PDMAEMA-*b*-PBzMA macro-CTA already self-assembled into micelles, worms and vesicles.[112] Phase segregation of PTHFOMA and PBzMA block copolymers were evidenced by the formation of compartmentalized nanostructures. An abundant variety of segregated morphologies were observed such as patchy, ribbon-shell and raspberry-like micelles (Fig. 9). The morphology evolution of these multi-compartment micelles (MCM) was controlled by the lengths of the PBzMA and PTHFOMA blocks. A series of PISA formulations based on semi-fluorinated methacrylates with different fluorinated side-chain lengths (C_4F_9 NFHMA, C_6F_{13} THFOMA, C_8F_{17} FDMA) was reported by the same team.[113] Among their findings they highlighted that only spheres could be prepared when PTHFOMA was used as the core forming block. Elongated cylindrical micelles could be obtained when FDMA was used presumably because of the liquid crystalline nature of FDMA.

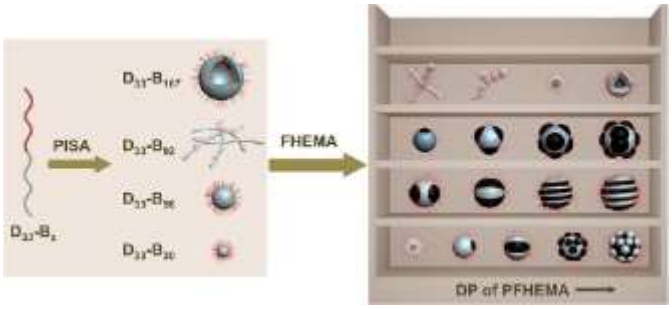

Fig. 9. (left) Schematic representation of the PISA process and resulting morphologies obtained in the course of the preparation of PDMAEMA-*b*-PBzMA micelles, worm-like and vesicles seeds. (right) Compartmentalized nanostructures with large variety of morphologies as function of DP pf PFHEMA (coined PTHFOMA in the text). Color code: D (red, PDMAEMA), B (grey, PBzMA), and H (black, PTHFOMA). Reproduced with the permission from ref. [112] ACS 2017 Copyright.

The same authors also reported one-pot PISA synthesis of PDMA-*b*-PBzMA-*b*-PFDMA triblock copolymers in ethanol (Fig. 10a).[114]

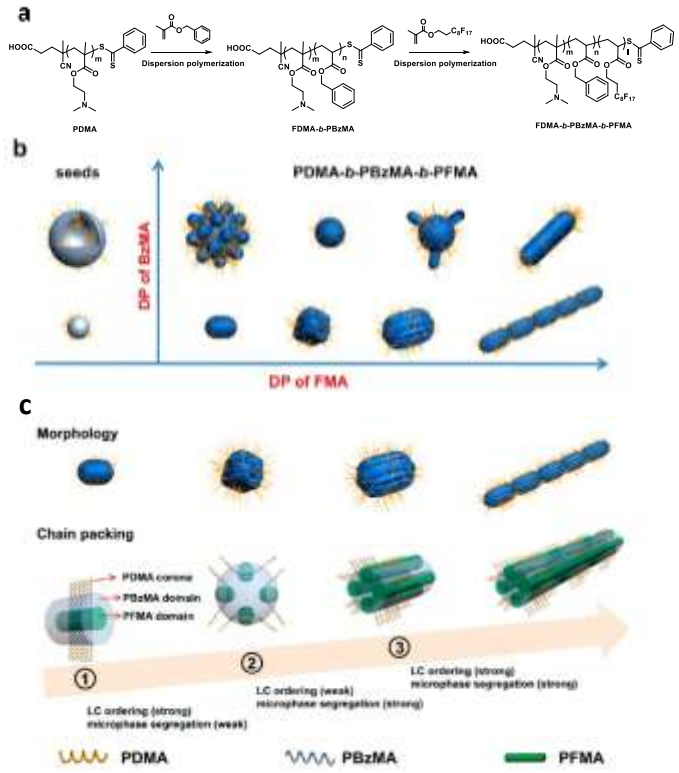

Fig. 10. a) Synthetic route utilized for the preparation of PDMA-*b*-PBzMA-*b*-PFDMA triblock copolymers. b) Schematic representation of the obtained morphologies as a function of BzMA and PFDMA (FMA) degree of polymerization (DPn). c) Proposed mechanism for the formation of LC ordered morphologies with the increasing PFDMA block length: $PDMA_{33}$-*b*-$PBzMA_{58}$-*b*-$PFDMA_{16,30,62,120}$ (from left to right). Adapted with the permission from ref. [114]. ACS 2017 Copyright.

Upon variation of the chain lengths of PBzMA and PFDMA (also called PFMA), the authors observed different morphology evolution which were attributed to the interplay of the hydrophobic interactions among the PBzMA blocks, the lipophobic interaction, and the LC ordering of the PFDMA blocks (Fig. 10 b and c). This system was later optimized and explored in details by the same group.[115–117] Recently, ICAR ATRP under PISA conditions was also used to prepare organic–inorganic

hybrid nanoparticles (ICAR = initiators for a continuous activator regeneration).[118] The fluorinated block (PFDMA) was used to tune the solubility of the copolymers, while glycidyl methacrylate (GMA) provided reactive epoxy groups that were later used for surface modification. By modulating the solids content as well as the GMA/ THFOMA molar ratio, various morphologies such as spheres and short worms were achieved.

2.2.15. Pentafluorophenyl (meth)acrylates (PFP(MA))

Perfluorinated alkyl methacrylates have been relatively well investigated probably because they offer the possibility of modulating their hydrophobicity/fluorophilicity ratio via varying the length of the fluorinated chain. In comparison, pentafluorophenyl methacrylates were more rarely studied. However, they have gained attention because of the selective reactivity of the para position providing an attractive and efficient tool for chemical post-modification.[119–122] Indeed, every types of thiols (primary, secondary, and tertiary as well as aliphatic and aromatic thiols) have shown to effect the substitution of the fluorine atom on the para position, while the pentafluorophenyl activated ester group, is known to efficiently react with amines to form amides. The PISA of pentafluorophenyl methacrylates was pioneered by the Lowe group in 2015, who reported the preparation of fluorinated polymethacrylate copolymer self-assembled nanoobjects via RAFT dispersion polymerization in ethanol.[123] Aggregates with common morphologies such as spheres, worms, and vesicles were obtained. These particles were then chemically modified using a thio-sugar. This modification resulted into identical morphologies or minor changes such as mixed phases of spheres and worms. Following this methodology, the same group also prepared other fluorinated soft nanoparticles of various morphologies.[124] Using a copolymer of stearyl methacrylate (SMA) and pentafluorophenyl methacrylate (PFPMA), they performed RAFT dispersion polymerization of 3-phenylpropyl methacrylate (PPMA) in *n*-octane or *n*-tetradecane. TEM images showed typical PISA morphologies. The reactive pentafluoro methacrylate units were then modified into acrylamide via acyl substitution reaction with primary amine. Using a similar approach but by using para-fluoro substitution with thiols), Roth and co-workers prepared cross-linked particles,[125] or induced morphological transitions.[126] In this latter example, PEGMA-*b*-PFBMA diblock copolymers prepared via RAFT dispersion polymerization in ethanol generated either spherical or worm-shaped morphologies that were modified, post-synthesis, with a selection of 15 different thiols through thiol–parafluoro substitution reactions in the nano-object cores. Depending on the choice of thiol, spherical nano-objects underwent an order–disorder transition to form unimers, increased in size, or underwent an order–order transition to form worm-shaped nano-objects. These morphological transitions were ascribed to the modification of the packing parameters caused by the change in the solvophobicity brought about by the grafted thiol moieties.

3. Poly(fluorinated styrene)-based copolymers

The self-assembly of fluorinated styrene-based BCP was pioneered by the Laschewsky group with an ABC poly(4-methyl-4-(4-vinylbenzyl)morpholin-4-ium chloride)-*b*-polystyrene-*b*-poly(pentafluorophenyl 4-vinylbenzyl ether) (PVBM-*b*-PS-*b*-PVBFP) linear triblock copolymer.[127] This triblock copolymer was prepared by quaternization of a poly(vinylbenzyl chloride)-*b*-PS-*b*-PVBFP precursor (synthesized by RAFT polymerization) with *N*-methylmorpholine. The triblock copolymer was dispersed in a dioxane/water binary mixture and self-assembled using method 7. Cryo-TEM images revealed the presence of 20–30 nm multicompartment micelles with cores segregated into nanometer-sized compartments containing small fluorocarbon-rich domains coexisting with the continuous hydrocarbon-rich region (Fig. 11).

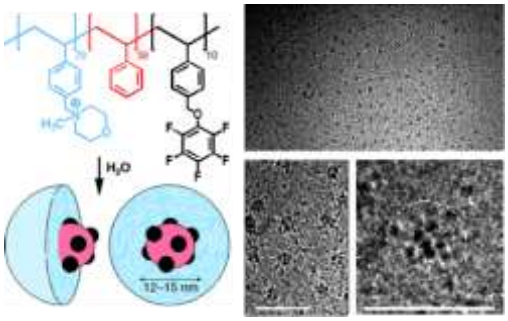

Fig. 11. Structure of PVBM-*b*-PS-*b*-PVBFP triblock copolymer, cryo-TEM images, and schematic representation of multicompartment micelles arising from the self-assembly in water. The corona of the micelles is not visible. The scale bars correspond to 50 nm. Adapted with the permission from ref. [127]. Wiley-VCH 2005 Copyright.

In another report, the complexation of polyanionic blocks with multivalent counter cation were used to obtain polyion complex (PIC) micelles that underwent local intra-micellar phase separation.[128] Polystyrene (PS) and poly(2,3,4,5,6-pentafluorostyrene) (PPFS) were employed as the third hydrophobic block in PAA-*b*-PMA-*b*-PS and PAA-*b*-PMA-*b*-PPFS. Equal molar amounts of these two triblock copolymers were dissolved in pure THF. A diamine (1:1 molar ratio with PAA) was added to complex the PAA block and induce the formation of the PIC micelle. In the next step, the addition of water (THF:water = 1:2) triggered the formation of cylindrical micelles. The incompatibility of PS and PPFS resulted in nano-phase separation producing multicompartment micelles with pronounced undulations along the cylinder surfaces (Fig. 12).[128]

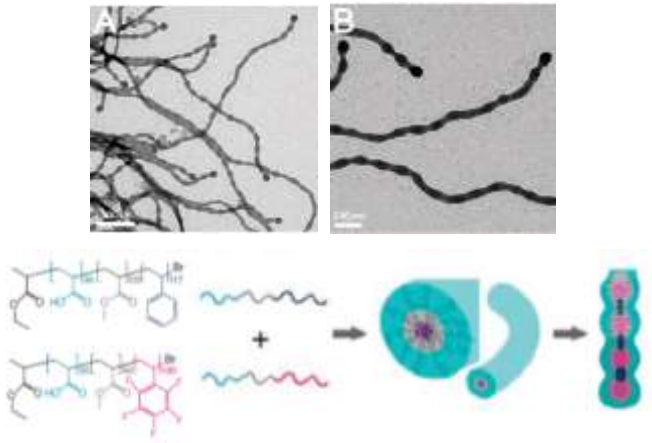

Fig. 12. (top) Nanostructured multicompartment cylinders. (A and B) Bright-field TEM images with dark regions standing for PPFS-chain rich area (bottom) Schematic illustration of formation of multicompartment cylinders. Adapted with the permission from ref. [128] Copyright 2007 AAAS.

In 2008, the Davis group reported the RAFT synthesis of a pH-responsive amphiphilic PDMAEMA-*b*-PPFS block copolymer.[129] The micelle formation, in water using method 1, was investigated by fluorescence spectroscopy, Static Light Scattering (SLS), DLS, and TEM. DLS and SLS measurements revealed that the diblock copolymers formed spherical micelles with large aggregation numbers where the dense PPFS cores were surrounded by PDMAEMA chains. The hydrodynamic radii R_h of these micelles at pH 2–5 were larger as the protonated PDMAEMA segments swell the micelle corona. R_h decreased as the pH increased due to increasing hydrophobicity. Nonetheless, the radius of gyration (R_g) remained pH independent as the PPFS core is not pH-responsive. In a parallel study, the same group synthesized well-defined fluorinated brush-like amphiphilic diblock copolymers of PPEGMA and PPFS by ATRP and self-assembled those copolymers using method 1.[130] The hydrodynamic radius (R_h) of the micelles in aqueous solution was in the nanometer range, regardless of the polymer concentration. Diblock copolymers with longer PPEGMA block (DP= 19) formed micelles with smaller R_h and lower aggregation numbers. Interestingly, an increase in temperature induced the comb-like PEG segments in the corona to dehydrate and shrink (LCST behaviour, lower critical solution temperature), leading to the formation of micelles with larger aggregation numbers.[130] The same authors also reported the synthesis, micelle formation, and bulk properties of semifluorinated amphiphilic PEG-*b*-PPFS-*g*-POSS (POSS:polyhedral oligomeric silsesquioxane) copolymers.[131] The synthesis of PEG-*b*-PPFS diblock copolymer was achieved via ATRP using a poly(ethylene glycol)-based macroinitiator. Subsequently, a fraction of the reactive fluorine atom on the para position of the PPFS units was replaced with amino-functionalized POSS through aromatic nucleophilic substitution reaction. The products, PEG-*b*-PPFS and PEG-*b*-PPFS-*g*-POSS, were self-assembled in aqueous solutions using method 3. The CMC (critical micelle concentration) of these polymers decreased concomitantly with the number of POSS particles grafted per copolymer chain. Wooley's group[132] prepared, via a relatively complex synthetic procedure consisting of self-condensing ATRP of an inimer: 1-(40-(bromomethyl)-benzyloxy)-2,3,5,6-tetrafluoro-4 vinylbenzene, amphiphilic hyperbranched fluoropolymers that formed nanometric micelles. Tan et al.[133] synthesized a series of amphiphilic copolymers by radical copolymerization of sodium 2-acryamido-2-methylpropanesulfonate and styrene derivatives with a fluorocarbon side chain (3,3,4,4,5,5,6,6,7,7,8,8,8,-tridecafluoro-1-octanol). Their self-assembly in aqueous solution using method 1, indicated that the self-assembly and the surface activity depended on the fluorocarbon content of the copolymer. Since 2019, these fluorinated copolymers have gained attention especially for preparation of internally ordered morphologies such as cubosomes and nanotubes.[19] Lv et al.[134] prepared various self-assembled morphologies of PDMA-*b*-(P(S-*alt*-PFS)) block copolymers prepared by PISA using a PDMA (polydimethylacrylamide) macro-CTA. At DP<300 for the P(S-*alt*-PFS) block, common morphologies (spheres, worms and vesicles) were observed. When higher DPs (428 or 582) were targeted, cubosomes with Im3m and P6mm mesophases were obtained. The formation of such morphologies was attributed to both high solids content and the short PDMA stabilizer block, facilitating the inelastic collision between particles, resulting in the formation of higher order morphologies. Addition of a small fraction of co-solvent at high monomer conversions (acting as plasticizer), facilitated the chain mobility and morphological transition. The addition of a co-solvent to promote plasticity was also used to prepare BCP nanotubes.[135] PDMA-*b*-PPFS BCP morphologies were prepared by performing PISA in ethanol, and DMF was added to promote the nanotube formation (Fig. 13). Through several experiments, this study showed that the nanotube formation was governed by T_p, (polymerization temperature), and T_{sg} (glass transition temperature) of the solvated cores. Formation of nanotubes was highly favoured when T_p was lower than or close to T_{sg}.

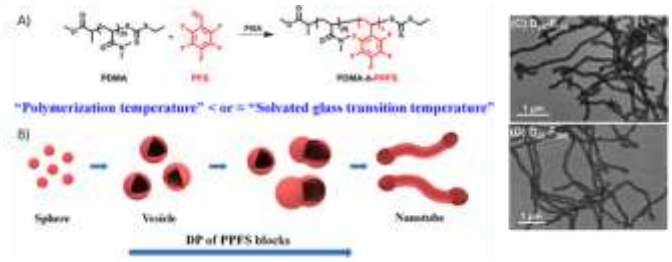

Fig. 13. A) Chemical structure of PDMA-*b*-PPFS block copolymer prepared by RAFT PISA. B) Morphologies evolution of PDMA-*b*-PPFS block copolymer through PISA process with $T_p \approx T_{sg}$ or $T_p < T_{sg}$. C) and D) Nanotubes morphologies obtained for $PDMA_{29}$-*b*-$PPFS_{180}$ and $PDMA_{29}$-*b*-$PPFS_{200}$ at 30% w/v solid content in 5% DMF/ethanol (T_p and T_{sg} = 65 °C). Adapted with the permission from ref. [135]. ACS 2020 Copyright.

4. Poly(perfluoropolyethers)-based copolymers (PFPE)

4.1. PFPE-based miktoarm triblock copolymers

The ABC miktoarm (μ-ABC) star terpolymer architecture provides a versatile and powerful route toward multicompartment micelles. Because of the mandatory

convergence of three blocks at a common point, the miktoarm star architecture suppresses the formation of the default core/shell/corona "onion-like" arrangement often adopted by linear ABC triblock terpolymers. This promotes segregation of all three mutually immiscible polymer chains at their contact point. In 2004, Lodge et al.[136] reported the observation of multicompartment micelles prepared from a miktoarm star polymer comprising water-soluble poly(ethylene oxide) (PEO) arm and two hydrophobic immiscible components, poly(ethylethylene) (PEE) and poly(perfluoropropylene oxide) (PFPO). These μ-(PEE)(PEO)(PFPO) star triblock copolymers, abbreviated μ-EOF, were prepared using two successive anionic polymerization steps and one polymer-polymer coupling reaction.[137] Different types of multicompartment micellar structures were identified in dilute aqueous solution depending on the composition of the μ-EOF star triblock copolymers,[138] as revealed by cryogenic transmission electron microscopy (Fig. 14). The observed micellar structures were generally correlated with the O (PEO) corona size and the relative length of the E (PEE) and F (PFPO) blocks. The strong incompatibility of the three polymeric components drove the formation of segregated micelle cores even at modest molar mass. The extreme hydrophobicity of the F block placed the system in the superstrong segregation regime[139] within which the interfacial tension is so large that the minority core-forming block is essentially completely extended and the interfacial area per chain is minimized. Upon decreasing the length of the O block, the resulting micelles evolved from "hamburger" micelles to segmented worms and ultimately to nanostructured bilayers and vesicles (Fig. 14). When the F block was the minority component, segmented ribbons, Y -junctions, and networks were preferred.

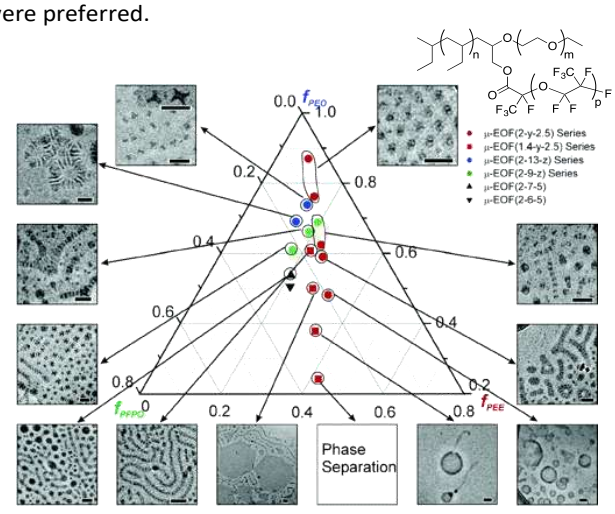

Fig. 14. Multicompartment micelle morphology diagram for μ-EOF miktoarm star terpolymers in dilute aqueous solution as a function of composition. f_{PEE}, f_{PEO}, and f_{PFPO} are the volume fractions of the PEE, PEO, and PFPO blocks, respectively. They are designated μ-EOF(x-y-z), where x, y, and z represent the E, O, and F block molar masses, respectively, in kD. Reproduced with permission from ref [138]. Copyright 2006 ACS.

A longer F block compared to the E block, resulted in formation of novel morphologies such as raspberry-like micelles and multicompartmentalised worms.[140] Solvent selectivity was also shown to be an efficient way to reach various micellar morphologies with miktoarm star μ-EOF micellar systems. By incorporating a good solvent for the E block (e.g. THF) into aqueous dispersions of a μ-EOF block, the micellar structure evolved from multi-compartment disks to core shell corona worms, spheres and finally to mixed corona (E + O) oblate ellipsoidal micelles with increasing THF content.[141] Using a μ-ABC/AB blend, the same authors reported the formation of "hamburger" micelles from EO diblock copolymers (forming spherical micelles) and μ-EOF miktoarm star terpolymers (forming segmented worm-like micelles).[142] This morphological evolution most probably occurred via the collision/fusion/fission mechanism whereby the long μ-EOF segmented worm-like micelles first fused with EO spherical micelles, followed by fission, giving progressively shorter micelles, which finally evolved into more stable hamburger-like micelles. To date, the use of multicompartment micelles for nanotechnology applications that utilize their inherent storage and release capacities remains limited. The Lodge group has demonstrated the possibility of using μ-EOF-based multicompartment micelles to solubilize two distinct hydrophobic dye molecules within two separate nano-sized compartments.[143] Crucially, these findings indicate that there is little relationship between the distinct solubilization efficiencies and therefore simultaneous or sequential storage and release of two different hydrophobic payloads could be possible.

4.2. PFPE-based miktobrush terpolymers

In 2016, Hillmyer's group reported the aqueous self-assembly of μ-A(BC)n miktobrush terpolymers synthesized using RAFT polymerization.[144] In this system, the A block (attached to the R-group of the RAFT CTA) was hydrophilic PEO (O). The B block was hydrophobic PMCL (C), and the C block was hydrophobic/oleophobic PFPO (F), both in the form of a macromonomer polymerized using the PEO-modified CTA. The aqueous self-assembly of μ-O(CF)n miktobrush terpolymers were characterized using DLS and cryo-TEM. The first terpolymer investigated (f_{PEO} = 0.63, f_{PMCL} = 0.28, f_{PFPO} = 0.09) formed hamburger and evolved over time to raspberry-like micelles (likely due to the large volume fraction of PEO). This transition seemed to be attributed to partial solvation of PEO by PMCL chains which induced a larger volume fraction of PEO. Within the hamburger micelles, the PMCL chains formed the "buns" around an oblate PFPO core disk, thereby decreasing the interfacial penalty between the PFPO domains and the solvated PEO blocks. These findings are broadly consistent with their previous findings on μ-EOF and μ-EOC miktoarm star terpolymer systems.[136,138,144] The μ-O(CF) terpolymer (f_{PEO} = 0.57, f_{PMCL} = 0.35, f_{PFPO} = 0.08) formed multilamellar vesicles or polymersomes with nanoscopic periodicity within their bilayer, because of dispersed PFPO domains within the PMCL matrix.

4.3. PFPE-based linear block copolymers

Thüneman et al.[145] synthesized a symmetrical linear ABCBA pentablock copolymer consisting of: (A) PEO, (B) poly(γ-benzyl L-glutamate) (PBLG), and (C) a perfluoropolyether (PFPE, Fluorolink® C). The diblock copolymer PEO-*b*-PBLG was

synthesized by ring-opening polymerization of the *N*-carboxy anhydride of *γ*-benzyl-*L*-glutamate using ammonium chloride-functionalized PEO as the macroinitiator. In a second step, the PEO-*b*-PBLG diblock was covalently coupled to an α,ω-dicarboxyl-PFPE via a carboxyl-amine reaction. The different blocks were highly immiscible and formed two-compartment cylindric micelles in aqueous solution. In 2006, Lodge et al.[146] reported the first example of a coil-coil nonionic diblock copolymer adopting a flat disk morphology. The diblock copolymer was synthesized through the coupling reaction of hydroxy-terminated 1,2-polybutadiene and acid-chloride-end-functionalized PFPE (Krytox® 157-FSH). Both blocks were atactic, noncrystalline, and flexible (low Tg). The micellization was performed in bis(2-ethylhexyl) phthalate, selective solvent for polybutadiene. The self-assembled thin disk micelles, had radii ranging from 20 to 150 nm and core thickness of approximately 10 nm. The adopted morphology was clearly the result of an unusually significant interfacial tension between the fluoropolymer and the solvated polybutadiene block. The same authors studied the self-assembly of two PFPE-based triblock copolymers, BOF and FOF.[147,148] First, a hydroxy-terminated poly(1,2-butadiene)-*b*-poly(ethylene oxide) (BO) diblock copolymer was synthesized by two successive living anionic polymerizations. Carboxylic acid end-capped poly(perfluoropropylene oxide) (PFPO-COOH) was converted to the acid chloride derivative by reaction with oxalyl chloride. The BOF triblock was obtained by coupling the hydroxy end-functional BO with the acid chloride end-functional PFPO. FOF was synthesized by reacting α,ω-dihydroxy-PEO with acid chloride end-functional PFPO. Aqueous gels formed from these polymers at concentrations ranging from 10 to 50 wt.% were investigated using cryogenic scanning electron microscopy (cryo-SEM) and SANS. The cryo-SEM micrographs revealed significant differences among the morphologies of the resulting gels, depending on the end-block used (Fig. 15). The FOF copolymer formed networks by aggregation of the end-blocks, but the PFPO blocks tended to adopt disk-like or even sheet-like structures. This was attributed to the significant interfacial tension of PFPO with water, consistent with the superstrong segregation regime. The heterotelechelic BOF terpolymers formed an intricate bicontinuous open-cell foam, with cell sizes around 500 nm with walls composed of PFPO disks embedded in PB sheets. These different network structures illustrate the potential of using end-block chemistry to control both the morphology and the physical properties of fluorinated polymer gels.

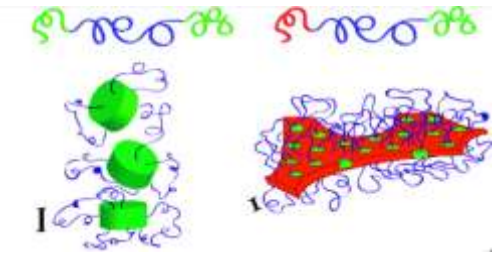

Fig. 15. Schematic representations showing the dependence of network morphology on the end-blocks. 1,2-Polybutadiene, poly(ethylene oxide), and poly(perfluoropropylene oxide) are shown in red, blue, and green, respectively. The scale bars represent 5 nm. Adapted with permission from ref. [147]. Copyright 2010 ACS.

Qiao et al. reported the synthesis of a perfluoropolyether-*b*-poly(*t*-butyl acrylate) ($PFPE_{1800}$-*b*-$PtBA_{8400}$) diblock copolymer in two steps.[149] A mono-hydroxy PFPE was reacted with 2-bromoisobutyryl bromide to form a macroinitiator containing a terminal bromine moiety. This ATRP macroinitiator was then used to polymerise *t*-butyl acrylate (*t*BA). Self-assembly of the resulting $PFPE_{1800}$-*b*-$PtBA_{8400}$ diblock copolymer was conducted in benzene (selective solvent of P*t*BA). DLS analyses revealed the formation of 400 nm monodispersed micelles. The diblock copolymer was also used to prepare honeycomb patterned films on both planar and non-planar surfaces via the Breath-figure technique using a static casting system.[149] Lopez et al. reported the synthesis of a PEG_{2000}-based amphiphilic triblock copolymer containing a $PFPE_{1200}$ central core that was synthesized by copper(I)-catalyzed alkyne–azide cycloaddition (CuAAC) between a telechelic alkyne PFPE and a PEG-azide.[150] The PEG_{2000}-*b*-$PFPE_{1200}$-*b*-PEG_{2000} triblock copolymer self-assembled into spherical micelles in aqueous solution with diameters of 10–20 nm. In 2007, Lodge et al. synthesized two polylactide-*b*-poly(perfluoropropylene oxide) diblock copolymers via coupling of acid chloride end-functionalized PFPOs and hydroxy-terminated PLAs.[151] The solubility of these materials in $scCO_2$ was measured using a variable-volume high-pressure cell. At a concentration of 1 wt %, the diblock copolymers were found to be soluble at modest pressures (< 500 bar) over the temperature range of 30–65 °C. The size of the resulting micelles in $scCO_2$ was characterized by high-pressure-DLS. These measurements indicated the formation of predominantly small, spherical micelles for PLA_{4000}-*b*-$PFPO_{6000}$ and large aggregates with hydrodynamic radii of 100 nm for PLA_{5000}-*b*-$PFPO_{4000}$. Vesicles were formed by kinetically trapping the aggregates in CO_2 through vitrification of the PLA cores and re-dispersing them in a PFPO selective solvent. This vesicles were later used in microfluidic devices which can find applications for in vitro translation, encapsulation and incubation of cells.[152] Spatz et al.[153] developed a novel approach to form biofunctionalized droplets of water-in-oil emulsions with the potential to serve as 3D APC (antigen-presenting cells) surrogates (Fig. 16). The PFPE-*b*-PEG-*b*-PFPE triblock copolymer (B, Fig. 16) was obtained using a one-step condensation reaction between PEG_{600}-diol and $PFPE_{2500}$-dicarboxylic acid. PFPE-*b*-PEG-Gold diblock surfactant (C, Fig. 16) was synthesized using a one-step condensation reaction between $PFPE_{7000}$-carboxylic acid and (11-mercaptoundecyl)-tetra(ethylene glycol)-functionalized gold nanoparticles. Two alternative approaches were adopted to test how efficiently the gold nanoparticles inside the droplets could serve as anchoring points and provide the required chemical and biological key functions of APCs. In 2020, Wang and team reported the synthesis of a symmetrical ABA-triblock copolymer containing a middle perfluoropolyether block via ATRP using a difunctional PFPE macroinitiator. A series of poly(isobornyl methacrylate)-*b*-perfluoropolyether-*b*-poly(isobornyl-methacrylate) (PIBOMA-*b*-PFPE-*b*-PIBOMA) with fixed PFPE block length and different

PIBOMA block lengths were synthesized and self-assembled into micelles with PIBOMA core and PFPE corona in 1,1,2-trichlorotrifluoroethane/*N,N*-dimethylformamide (F113/DMF) binary mixture. These micelles were then used to prepare hydrophobic films (water contact angle of 155° and sliding angle of 4°) by solvent evaporation at ambient temperature.[154]

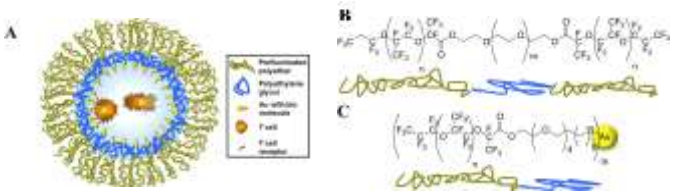

Fig. 16 A) Schematic representation of a nanostructured and specifically biofunctionalized drop of a water-in-oil emulsion as a 3D APC analogue. (B, C) Structures of the PFPE-*b*-PEG-*b*-PFPE triblock copolymers and PFPE-*b*-PEG-Gold diblock surfactants, respectively. Reproduced with permission from ref [153]. Copyright 2013 ACS.

5. Perfluorocyclobutyl (PFCB)-based copolymers

The chemistry of perfluorocyclobutyl polymers (PFCB) was developed by the Dow Chemical Company in the early 1990s.[155] David Babb pioneered the study of polymers containing 1,2-bisaryloxy-substituted perfluorocyclobutane (PFCB) ring.[155] PFCB ring-containing polymers with various macromolecular architectures such as linear, branched, and cross-linked are prepared by [2+2] cycloaddition of single molecules containing multiple aryl trifluorovinyl ether groups.[156] Typically, thermoplastic or thermosetting PFCB polymers can be obtained by simply heating aryl trifluorovinyl ether monomers in the bulk or in solution above 150 °C. The PFCB backbone contains equal numbers of randomly distributed cis- and trans-1,2-disubstituted hexafluorocyclobutanes. Initially developed for aerospace and microelectronics applications, PFCB polymers find use in microphotonics, coatings, nanocomposite dispersing matrix, hole transport layers for light-emitting diodes, cross-linking groups in electro-optic chromophores, and proton exchange membrane materials for hydrogen fuel cells.[157]

Self-Assemblies of amphiphilic PFCB-based copolymers were solely investigated by the group of Huang. In 2009, they reported for the first time, the synthesis and the self-assembly behaviour of a PFCB-based block copolymer.[158] A new PFCB-based methacrylate monomer (TPFCBBMA) was prepared in 5 steps from 4-methylphenol (Fig. 17). Well-defined PTPFCBBMA-*b*-PEG-*b*-PTPFCBBMA amphiphilic triblock copolymers were synthesized by ATRP of TPFCBBMA from telechelic PEG-based macroinitiator. These triblock copolymers had low solubility in water due to the significant content of hydrophobic TPFCBBMA moieties. For self-assembly, method 6 was employed. Spherical micelles were formed with a shorter hydrophobic block, while cylindrical micelles were observed when the block length of TPFCBBMA was increased. However, this morphology evolution was not evidenced with TEM images.

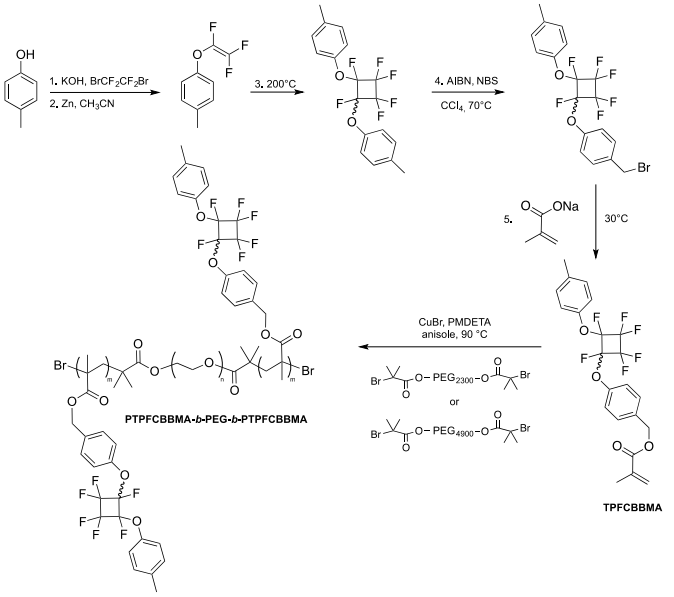

Fig. 17. Synthesis of PTPFCBBMA-*b*-PEG-*b*-PTPFCBBMA amphiphilic triblock copolymers as reported by Huang et al. [158].

The same group also reported the synthesis and the self-assembly of a series of well-defined semi-fluorinated amphiphilic diblock copolymers with hydrophilic PAA and fluorophilic PTPFCBBMA segments.[159] The PAA-*b*-PTPFCBBMA amphiphilic diblock copolymers were obtained via the selective acid hydrolysis of the poly(methoxymethyl acrylate) block. Method 3 was employed to trigger the self-assembly. Micellar morphologies were visualized by TEM. Diblock copolymers with short fluorophilic PTPFCBBMA blocks, formed spherical micelles and longer PTPFCBBMA blocks led to formation of pearl-necklace structure. They also demonstrated that the size of the micelles could increase with the increasing length of the PTPFCBBMA block.[160] In 2011, the same group reported the synthesis and self-assembly of a series of well-defined semi-fluorinated amphiphilic diblock copolymers with hydrophilic PDEAEMA and fluorophilic PTPFCBBMA segments.[161] First, RAFT homopolymerization of TPFCBBMA was initiated by AIBN using cumyl dithiobenzoate as the chain transfer agent. Then the resulting PTPFCBBMA macro-RAFT agent was used to mediate the RAFT polymerization of DEAEMA. Self-assembly method 6 resulted in the formation of well-ordered large spherical compound micelles (LCMs) with diameters of 400–600 nm. In 2014, they reported the synthesis of a series of well-defined ABA PBPFCBPMA-*b*-PIB-*b*-PBPFCBPMA triblock copolymers via ATRP.[162] The self-assembly (using method 2) behaviour of these triblock copolymers in *n*-hexane, acetone, and 1,1,1-trifluoroacetone was investigated by TEM (
Fig. **18**).

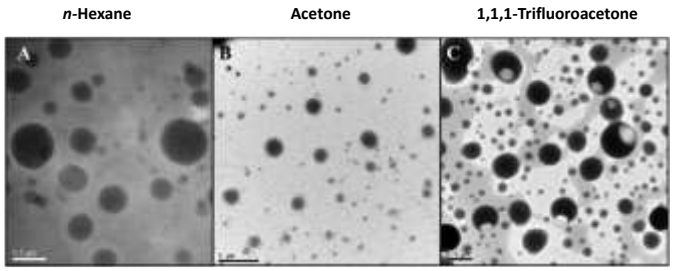

Fig. 18. TEM images of micelles formed by PBPFCBPMA-*b*-PIB-*b*-PBPFCBPMA triblock copolymers self-assembled in *n*-hexane (left), acetone (middle), and 1,1,1-trifluoroacetone (right). Adapted with permission from ref.[162]. Copyright 2014 RSC

The results indicated that spherical LCMs with PIB chain coronae were formed in *n*-hexane, whereas LCMs and bowl-shaped micelles with PBPFCBPMA block coronae were produced in acetone and 1,1,1-trifluoroacetone, respectively. They also reported the preparation of "sun-shaped" amphiphilic copolymers with PFCB aryl ether-based backbone and PAA lateral side chains.[163] The self-assembly in water of these polymers was achieved using method 6 and led to spherical micelles. In 2015, they synthesized a series of amphiphilic PFCB-based ABA triblock copolymers PDEAEMA-*b*-PBTFVBP-*b*-PDEAEMA.[164] A BTFVBP trifluorovinyl aryl ether monomer was first polymerized to form a semi-fluorinated perfluorocyclobutyl aryl ether-based segment, and end-functionalized to afford a Br-PBTFVBP-Br macroinitiator. Then, ATRP of DEAEMA was conducted in the presence of this difunctional initiator to afford PDEAEMA-*b*-PBTFVBP-*b*-PDEAEMA triblock copolymer. Self-assembly method 6 was used and spheres were formed in all process. Since the diameters of the spheres were much larger than the calculated extended length of the triblock copolymers, formation of LCMs was hypothesized. The authors speculated that the PBTFVBP segment formed the corona of the micelles and that their core was formed by numerous reverse micelles with islands of PBTFVBP in a continuous phase of PDEAEMA. LCMs were also obtained with $PDEAEMA_{36}$-*b*-$PBTFVBP_{27}$-*b*-$PDEAEMA_{36}$ and $PDEAEMA_{49}$-*b*-$PBTFVBP_{27}$-*b*-$PDEAEMA_{49}$ containing a more extended PBTFVBP segment (diameters ranging from 100 nm to 250 nm, Fig. 19, B and C). Conversely, $PDEAEMA_{22}$-*b*-$PBTFVBP_{27}$-*b*-$PDEAEMA_{22}$, with the lowest PDEAEMA/PBTFVBP ratio, self-assembled into vesicles of 300 nm in diameter (Fig. 19, A). As the initial water content was decreased from 30 wt.% to 10 wt.%, bowl shaped micelles with a diameter of about 500 nm were formed for $PDEAEMA_{36}$-*b*-$PBTFVBP_{27}$-*b*-$PDEAEMA_{36}$ (Fig. 19, D). Increasing the water content to 50 wt.% resulted in 100 nm spherical micelles (Fig. 19, E).

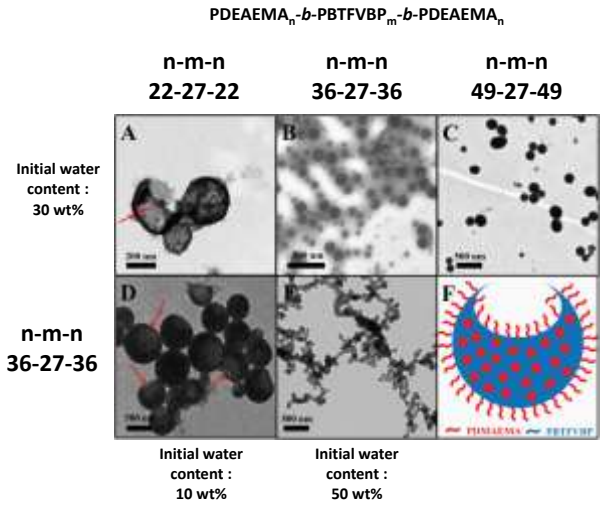

Fig. 19. TEM images of morphologies formed by three different PDEAEMA-*b*-PBTFVBP-*b*-PDEAEMA triblock copolymers self-assembled in water when varying the initial water content. Adapted with permission from ref. [164]. Copyright 2015 RSC.

The aforementioned team synthesized amphiphilic graft copolymers bearing a hydrophobic poly(2-methyl-1,4-bistrifluorovinyloxybenzene) (PMBTFVB) backbone and hydrophilic poly(ethylene glycol) (PEG) side chains.[165] The PMBTFVB was prepared by thermal step-growth cycloaddition polymerization of MBTFVB and sequential end-capping with 4-methoxy-trifluorovinyloxybenzene. The subsequent bromination of PMBTFVB with *N*-bromosuccinimide using benzoyl peroxide as the radical initiator at 80 °C yielded PMBTFVB-Br precursors. Then, PMBTFVB-*g*-PEG copolymers were synthesized through Williamson reaction between the hydroxyl end-group of PEG and the pendant benzyl bromide functionality of PMBTFVB-Br. Method 3 and 5 were employed to self-assemble this graft-copolymer in water. TEM images showed diverse morphologies such as spherical micelles, spindle micelles, and large compound vesicles depending on the solvent mixture water content, copolymer concentration and preparation method. They also reported the synthesis of amphiphilic graft copolymers bearing a hydrophobic poly(2-methyl-1,4-bistrifluorovinyloxybenzene) (PMBTFVB) backbone and (PAA) side chains.[166] PMBTFVB-*g*-PAA graft copolymers were synthesized by ATRP of *t*-butyl acrylate initiated by a PMBTFVB-Br macroinitiator followed by acidolysis of the hydrophobic P(*t*BA) side chains into hydrophilic PAA segments. Employing method 6, this graft-copolymer self-assembled into diverse morphologies including vesicular, worm-like, and bowl-shaped nanostructures, depending on the water content (from 25 to 70 wt.%) and the length of the PAA side chains. Vesicles (ca. 400–1100 nm) were formed in water:THF (25:75 wt.%) binary mixture at 1 g L^{-1} (Fig. 20, A1). The authors observed a 120 nm black dot at the centre of each vesicle that could be an artefact. A speculated explanation is that more polymer chains are found in the vesicle centre as the vesicle shells contract as a result of solvent evaporation during TEM sample preparation. In water:THF (50:50 wt.%) binary mixture, 250–500 nm bowl-shaped aggregates (Fig. 20, B1) and at lower water content

(25:75 wt.%), micrometer-long worm-like micelles (200 nm in diameter) were obtained (Fig. 20, A2). The addition of more water before dialysis (50 wt.% at 2 mg mL^{-1}) led to a network of worms (Fig. 20, B2). Decreasing the polymer concentration resulted in fewer polymer chains able to get into the micelle structure leading to lower aggregation number and facilitating the morphology transformation from bilayers (vesicles) to worm-like micelles.

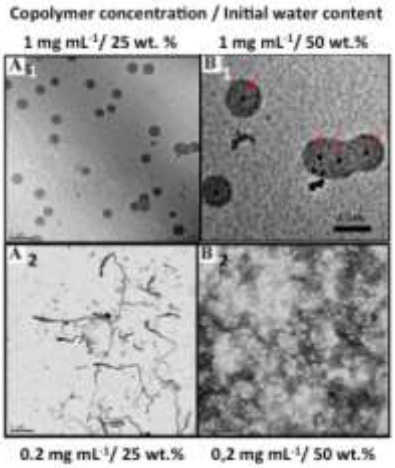

Fig. 20. TEM images of morphologies from PMBTFVB-*g*-PAA amphiphilic graft copolymers self-assembled in water when varying the initial water content and the concentration. Adapted with permission from ref. [166]. Copyright 2015 RSC.

6. Poly(2-oxazoline)-based copolymers

Poly(oxazolines) have been studied since 1960s, with a significant number of papers focusing on the polymerization of 2-substituted oxazolines.[167–170] Polymerizations are usually carried out via living cationic ring-opening mechanism (CROP), producing well-defined polymers and block copolymers with narrow average molar mass distributions.[171–174] Poly(2-oxazolines) with different properties can be prepared by varying the substituent on the monomers. In contrast to short alkyl side groups which provide water solubility, longer analogues and aromatic side chains lead to water-insoluble polymers. Amphiphilic systems are easily accessible and can be applied, for example, as micellar catalysts, nonionic surfactants, compatibilizing agent, and for the formation of hydrogels. However, the synthesis and self-assembly behaviour of fluorinated poly(2-oxazolines)-based copolymers have been scarcely investigated.

In 2008, Papadakis et al.[175] pioneered the synthesis and self-assembly of amphiphilic fluorinated poly(2-oxazolines)-containing block copolymers in water. Amphiphilic diblock copolymers of poly(2-methyl-2-oxazoline) (PMOx) as the hydrophilic block and poly(2-(1H,1H',2H,2H'-perfluorohexyl)-2-oxazoline) (PFOx) for the fluorophilic block were synthesized by sequential CROP. The synthesis of the PMOx-*b*-PFOx diblock copolymer was performed in an acetonitrile/chlorobenzene mixture using methyl triflate as the initiator and a three-fold excess of piperidine for termination (Fig. 21). Method 1 was employed to initiate the micellization in water. As judged by SANS and TEM, PMOx-*b*-PFOx formed elongated core/shell micelles. Schubert et al.[176] showed for the first time that well-defined gradient copolymers of 2-ethyl-2-oxazoline (EtOx) and 2-(m-difluorophenyl)-2-oxazoline (F2PhOx) can be prepared in one-pot under microwave irradiation (Fig. 21). These gradient copolymers featured an amphiphilic character inducing the formation of self-assembled micelles in aqueous solution using method 2. AFM and DLS characterizations of the micelles indicated that the copolymers formed spherical micelles with an average diameter of around 15 nm (AFM = Atomic Force Microscopy).

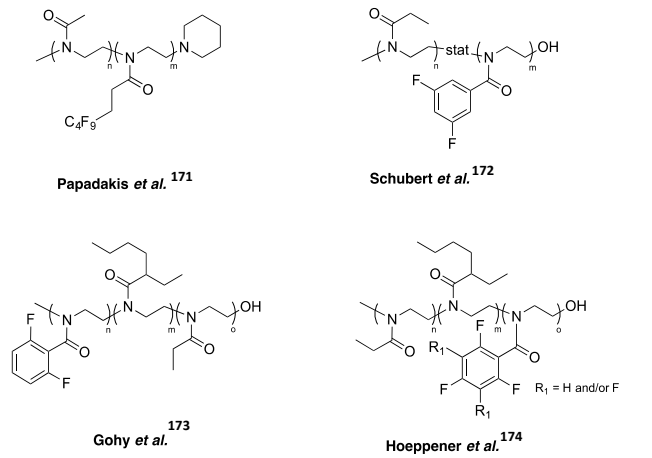

Fig. 21. Structures of self-assembled fluorinated poly(2-oxazolines)-based copolymers reported so far.

In 2010, Gohy et al.[177] reported the synthesis and self-assembly of a triblock copolymer containing a fluorinated poly(2-(2,6-difluorophenyl)-2-oxazoline) (PODFOx), a lipophilic poly(2-(1-ethylheptyl)-2-oxazoline) (PEPOx), and a hydrophilic PEtOx block (Fig. 21). Aqueous solutions of this PODFOx$_{23}$-*b*-PEPOx$_{28}$-*b*-PEtOx$_{49}$ triblock copolymer obtained via method 1 showed vesicles and flat aggregates of rolled-up cylindrical micelles coexisting in water (Fig. 22).

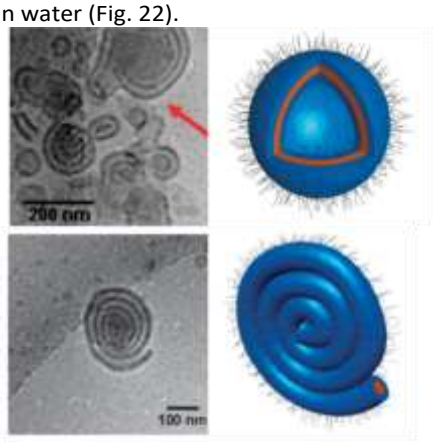

Fig. 22. Cryo-TEM pictures of micellar aggregates formed by the poly(ODFOx$_{23}$-*b*-EPOx$_{28}$-*b*-EtOx$_{49}$) triblock copolymer self-assembled in water. Adapted with permission from ref. [177]. Copyright 2010 RSC.

Based on the contrast observed in the cryo-TEM images and the fact that a mixture of PODFOx and PEPOx homopolymers demix

readily, the authors hypothesized that the vesicles consisted of segregated hydrophobic domains. The rolled-up spiral aggregates were proposed to be an intermediate metastable structure between cylindrical micelles and vesicles. Supposedly, the limited solubility of the PEtOx block in water induced further aggregation of the initially formed cylindrical micelles, while the low T_g of the PEPOx block provided sufficient flexibility for the cylindrical micelles to roll-up. These two structural parameters were believed to be the key factors driving the formation of the observed rolled-up hierarchical superstructures.

Based on the promising structural features of the aforementioned work, the same authors investigated the influence of the fluorophilic character on the formation of triblock copolymers aggregates.[178] For this purpose, a series of PEtOx-*b*-PEPOx-*b*-PXFPhOx (X = tri, tetra, penta) triblock copolymers were synthesized (Fig. 22). Cryo-TEM pictures revealed rod- and sheet-like morphologies for the trifluorophenyl-based triblock copolymers (Fig. 23, a and b). The authors proposed a mechanism of formation based on the strong hydrophobicity of the PTriFPhOx block and the stacking of the fluorinated phenyl rings caused by C-F dipole-dipole interactions. An increase of the number of fluorine atoms from PTriFPhOx to PTetraFPhOx block, resulted in better-defined shapes, with the presence of a few separated sheet-like structures and entangled rod-like features (Fig. 23, c and d). For PPentaFPhOx blocks, well-defined supramolecular structures were observed with perfectly round-shaped aggregates (Fig. 23, e and f). Further investigations revealed the presence of "onion-like" multilamellar vesicles with perfectly segregated concentric lamellar features. A large number of rod-like micelles were also observed alongside the well-defined complex "superaggregates."

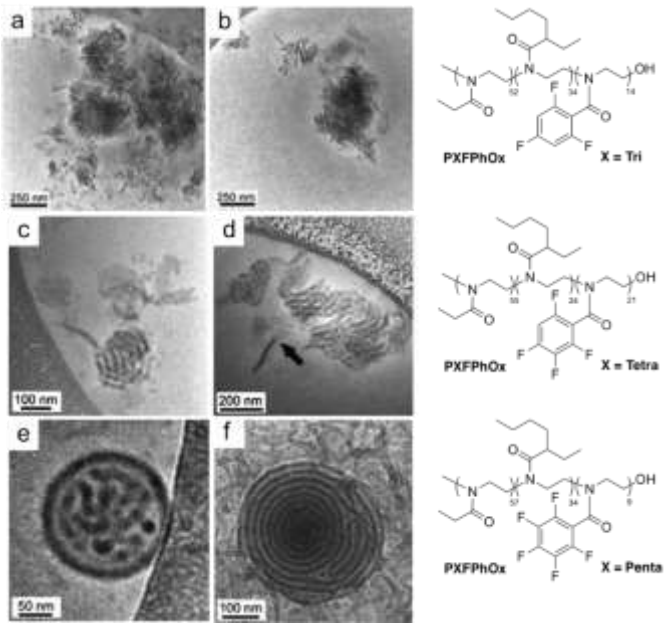

Fig. 23. Cryo-TEM pictures of micellar aggregates formed by PEtOx-*b*-PEPOx-*b*-PXPhFOx triblock copolymers self-assembled in water. Adapted with permission from ref.[178]. Copyright 2013 RSC

The ultimate thermodynamically stable structures (namely simple and multilamellar vesicles) were prepared by temperature-induced equilibrium. The absence of rod-like structure, led to the reasoning that the coexistence of bi-continuous and lamellar phases (non-equilibrium super aggregates) were a transition step towards the formation of more stable vesicular structures.

7. Miscellaneous

7.1. Fluorinated acrylamide

In 2013, Lee *et al.*[179] reported the synthesis of the thermoresponsive fluorinated polyacrylamide poly[*N*-(2,2-difluoroethyl)acrylamide]. The authors demonstrated that the thermosensitivity was easily controlled by changing the number of fluorine atoms in the terminal alkyl group of the *N*-ethyl moiety. Mono-substituted poly[*N*-(2-fluoroethyl)acrylamide] (P1F) was water-soluble while tri-substituted poly[*N*-(2,2,2-trifluoro-ethyl)acrylamide] (P3F) was water-insoluble. Interestingly, di-substituted poly[*N*-(2,2-difluoroethyl)acrylamide] (P2F) exhibited a LCST around 26–28 °C in water, which is comparable to that of poly-(*N*-isopropylacrylamide) (PNIPAM). In the continuation of this work, thermoresponsive double-hydrophilic fluorinated block copolymers were synthesized by RAFT.[180] First, poly[*N*-(2,2-difluoroethyl)acrylamide] (P2F) was synthesized *via* RAFT polymerization of *N*-(2,2-difluoroethyl)acrylamide (M2F) using 2-(Dodecylthiocarbono-thioylthio)-2-methylpropionic acid as the CTA. The resulting P2F macroCTA was further chain extended with *N*-(2-fluoroethyl)acrylamide (M1F) to yield poly{[*N*-(2,2-difluoroethyl)acrylamide]-*b*-[*N*-(2-fluoroethyl)acrylamide]} (P2F-*b*-P1F) diblock copolymers with different P1F lengths. Turbidimetry measured by UV- Vis spectroscopy, DLS, and *in situ* temperature-dependent ^{1}H NMR measurements demonstrated that the P2F block underwent a thermal transition from hydrophilic to hydrophobic, inducing the self-assembly of the unimers. TEM images demonstrated that polymeric aggregates formed from an aqueous solution of P2F-*b*-P1F at 60 °C were disrupted by cooling down to 20 °C and were regenerated by heating again to 60 °C. Temperature-triggered release of a model hydrophobic drug, coumarin 102, was also demonstrated.

In 2017, Jiang *et al.*[181] synthesized the monomer 2,2,2-trifluoroethyl 3-(*N*-(2-(diethylamino)ethyl)acrylamido)propanoate (TF-DEAE-AM) from *N*,*N*-diethylethylenediamine, 2,2,2-trifluoroethyl acrylate, and acryloyl chloride (Fig. 24).

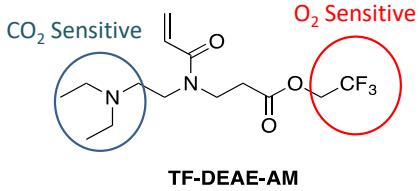

Fig. 24. Structure of TF-DEAE-AM monomer synthesized by Jiang et al.[181]

TF-DEAE-AM contains both O_2- and CO_2-responsive functionalities. Subsequently, a series of dual gas-responsive poly(TF-DEAE-AM) and PEG-*b*-poly(TF-DEAE-AM) were synthesized by RAFT and self-assembled in water using method 5. Due to the reaction between CO_2 and the DEAE groups, and the specific van-der-Waals interactions between O_2 and the trifluoromethyl groups, micelles consisting of poly(TF-DEAE-AM) or PEG-*b*-poly(TF-DEAE-AM) displayed distinct CO_2 and O_2 responsiveness in aqueous media. The authors demonstrated that pyrene (a model hydrophobic drug) could be encapsulated in the PEG-*b*-poly(TF-DEAE-AM) micelles. The release of pyrene was found to sharply increase after bubbling CO_2 or O_2 compared to N_2. Also the highest release rate was observed in solution treated with CO_2.

7.2. Fluorinated vinyl ether

In 1999, Yamaoka et al.[182] reported the synthesis of fluorine-containing block copolymers consisting of poly(2-hydroxyethyl vinyl ether) (PHOVE) and poly(2-(2,2,2-trifluoroethoxy)ethyl vinyl ether) (PTFEOVE). PHOVE-*b*-PTFEOVE diblock copolymers were synthesized by living cationic polymerization and subsequent hydrolysis. The formation of block copolymer micelles in water using method 1 was confirmed by SAXS measurements. Analysis of the SAXS profiles revealed the micelles had a core-shell spherical morphology and the aggregation number increased when increasing the length of PTFEOVE segment. Solubilization experiments revealed that PHOVE-*b*-PTFEOVE BCP had a higher ability to solubilize fluorinated compounds than non-fluorinated amphiphilic BCP. The same authors confirmed this finding when they reported the synthesis and self-assembly of amphiphilic ABA (PHOVE-*b*-PFPOVE-*b*-PHOVE) (HFH), and (PFPOVE-*b*-PHOVE-*b*-PFPOVE)] (FHF) (with PFPOVE standing for poly(2-(2,2,3,3,3-pentafluoropropoxy)ethyl vinyl ether) triblock copolymers,.[183] SAXS measurements revealed that HFH formed core-shell spherical micelles at 1 wt.% in aqueous solutions, whereas FHF formed more complex morphologies. In 2004, the same group reported the synthesis and self-assembly of PHOVE-*b*-PTFEOVE, PHOVE-*b*-PFPOVE, and PHOVE-*b*-HFBOVE diblock copolymers (with HFBOVE standing for poly(2-(2,2,3,3,4,4,4-heptafluorobutoxy)ethyl vinyl ether).[184] SANS, SAXS, and DLS analyses revealed that block copolymers bearing larger fluorinated groups were more likely to form rod-like micelles without much influence on the cross-sectional radii of the micelles. Scattering analysis of the copolymer micelle solutions containing hydrophobic dyes suggested that the dye solubilization strongly affected the micelle structures. The micelles became smaller as the solubility of the dye increased.

7.3. Fluorinated poly-ene

Müller et al.[185] reported the synthesis and self-assembly of fluorinated triblock copolymers derived from poly(4-tert-butoxystyrene)-*b*-polybutadiene-*b*-poly(tert-butyl methacrylate), (PtBS-*b*-PFB-*b*-PtBMA). The terpolymers were synthesized by fluorination of the PB block of PtBS-*b*-PFB-*b*-PtBMA by radical thiol-ene reaction of the vinyl groups with 1-mercapto-1H,1H,2H,2H-perfluorooctane. These fluorinated copolymers were then self-assembled in dioxane via direct dissolution (method 1). Spherical micelles were formed due to microphase separation of PtBS and PtBMA domains. Replacing dioxane with ethanol (selective solvent for PtBMA) following method 7, produced undulated bamboo-like cylindrical assemblies. Surprisingly, the cylinders were connected to each other with junctions that formed giant branched assemblies. Furthermore, the solvent-driven morphological transition between spheres and branched bamboo like morphologies was fully reversible.

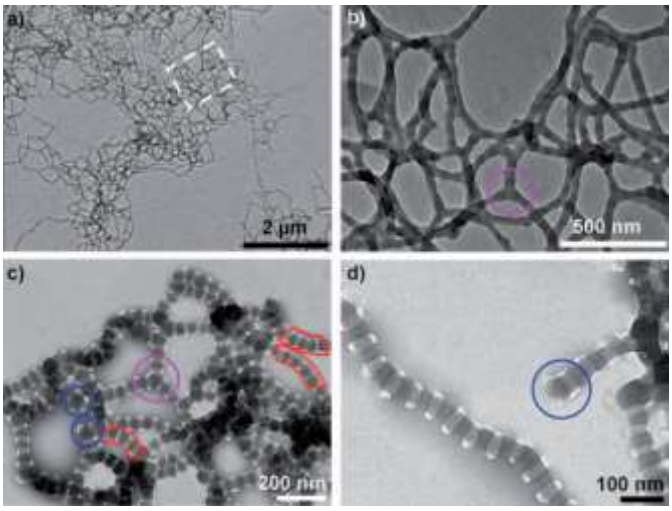

Fig. 25. a, b) Nonstained and c, d) RuO_4 stained TEM images of undulated cylinders obtained from ethanol dialysis of (PtBS-*b*-PFB-*b*-PtBMA) block copolymers particles in dioxane. Adapted with permission from ref.[185]. Copyright 2009 Wiley.

In 2011, Mays et al.[186] reported the synthesis and self-assembly of sulfonated polystyrene-*b*-fluorinated polyisoprene (sPS-*b*-fPI) BCP. PS-*b*-fPI block copolymers were synthesized by anionic polymerization, followed by fluorination and sulfonation. Self-assembly was achieved in water employing method 6, and the resulting aggregates were examined by TEM. sPS-*b*-fPI with 38.8 % of sulfonation formed worm-like nanostructures, which changed from ribbon-shaped to tapered structures as the sample aged (one week to one month). The diblock copolymer with 29.6 % of sulfonation exhibited similar morphologies, although the micelles appeared to be stiffer. The authors suggested that the higher sulfonation degree softened the assembled structure due to the increased solubility of the corona-forming chains in water.

7.4. Fluorinated polyphosphazene

In 2015, Presa-Soto et al.[187] reported the preparation of stable giant unilamellar vesicles (GUVs, diameter ≧ 1,000 nm) and large vesicles (diameter ≧ 500 nm) by self-assembly of crystalline-*b*-coil poly(di(2,2,2-trifluoroethoxy)phosphazene)-*b*-poly(methylphenylphosphazene) ($[N=P(OCH_2CF_3)_2]_n$-*b*-$[N=PMePh]_m$, PTFEP-*b*-PMPP, n=30/m=20, n=90/m=20, or n=200/m=85) diblock copolymers in THF. This block copolymer combined crystalline but flexible PTFEP and amorphous PMPP blocks. SEM, TEM, and WAXS experiments demonstrated that

the stability of these GUVs was caused by the crystallization of the PTFEP blocks in the walls of the GUVs. Higher degrees of crystallinity of the GUV walls were observed in the larger vesicles. This suggested that the crystallinity of the PTFEP block facilitated the formation of large vesicles. The GUVs were responsive to strong acids and, after selective protonation of the PMPP block, they underwent a morphological transition to smaller spherical micelles within which the core and corona were inverted. This morphological evolution was completely reversible upon neutralization with a base, regenerating the original GUVs (Fig. 26).

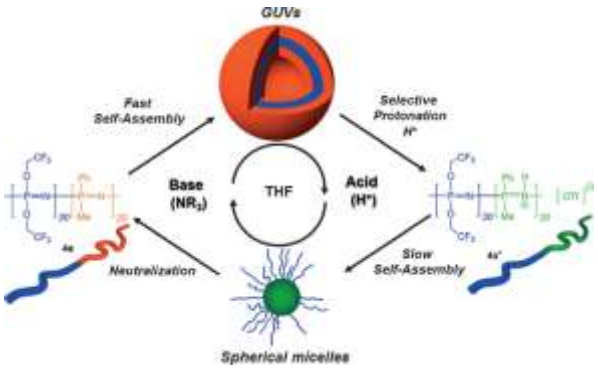

Fig. 26. Schematic representation of the reversible morphological evolution from GUVs to spherical vesicles, promoted by a selective acid–base reaction. Reproduced with the permission from ref. [187]. Copyright 2015 Wiley.

The same group also showed that bicontinuous nanospheres or toroidal micelles could be produced by the self-assembly of a single crystalline-*b*-coil (PTFEP-*b*-PS) diblock copolymer in THF (without additives), by simply adjusting the block copolymer concentration.[188] Moreover, these two rare morphologies were reversibly transformed one into the other in THF, by simple dilution (adding THF) or concentration (evaporating THF) of the block copolymer solution. The crystallinity of the core-forming PTFEP block appeared to be the main driving-force for the formation of the bicontinuous nanospheres and toroidal micelles. Hence, self-assembly of a linear PTFEP-*b*-PS diblock copolymer to form bicontinuous or toroidal micelles can be controlled by modulating the crystallization of the PTFEP segments by simply changing the block copolymer concentration.

7.5. Fluorinated siloxane

In 2012, Perahia *et al.*[189] reported the self-assembly of a poly(semi-fluorinated siloxane)-containing diblock copolymer, poly(trifluoro propyl methylsiloxane)-*b*-polystyrene (PSiF-*b*-PS) in toluene (a selective solvent for PS). The high incompatibility of the PSiF block drove the aggregation. For example, the symmetric triblock copolymer formed elliptical micelles with unique temperature stability compared to the aggregates formed by diblock copolymers in the lower segregation regime. The micelles had a relatively low aggregation number and contained high amounts of solvent in their core. As expected, the curvature of the core–corona interface was significantly affected by the volume fraction of the PSiF block.

In 2015, Manners *et al.*[190] investigated the self-assembly of diblock copolymers containing a crystalline poly(ferrocenyldimethylsilane) (PFS) block and a poly(fluorinated siloxane) coil block (PFMVS = poly(methylvinylsiloxane) with 1*H*,1*H*,2*H*,2*H*-perfluorooctane dangling chains). Direct dissolution (method 1) of the block copolymer in trifluorotoluene (TFT) did not result in the formation of any aggregates, even after 24h. However, when the polymer solution was allowed to stand for 1 week, cylindrical micelles with PFS cores were formed (Fig. 27).

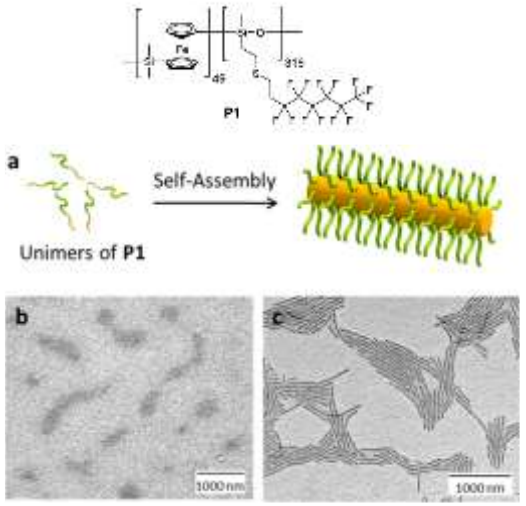

Fig. 27. Schematic representation of the self-assembly of PFS-*b*-PFMVS leading to cylindrical micelles. PFS = yellow, PFMVS functionalized with perfluoroalkane = light green (a). TEM micrographs of a drop-cast sample in TFT (60 mg/mL) after 24 h (b), and 1 week (c). Reproduced with the permission from ref. [190]. Copyright 2015 ACS.

Self-seeding protocols were also successfully employed to prepare micelles with controlled lengths and structures and low polydispersities. Finally, partial functionalization of the PFMVS block copolymers with a fluorescent dye, led to the formation of well-defined, functional nanomaterials.

In 2015, Dong et al.[191] reported the solution self-assembly of an ABC block terpolymer consisting of a polystyrene-*b*-poly(ethylene oxide) (PS-*b*-PEO) diblock copolymer tail tethered to a fluorinated polyhedral oligomeric silsesquioxane (FPOSS) cage. This terpolymer was self-assembled in 1,4-dioxane/water binary mixture using method 2. At low water content (10 wt %), spherical micelles with uniform size distributions were produced. A sphere to worm transition was observed when the water content increased to 18 wt. %. Other circular morphologies were formed at water contents ranging from 22 to 34 wt. %, including toroids (**Fig. 28**, a), tadpoles and dumbbells (**Fig. 28**, b), interlocked toroids (**Fig. 28**, c), etc. Toroid was the prevalent morphology. These toroidal structures had similar diameter and identical core-shell-corona molecular arrangement as the worm-like micelles. For this reason, they were supposed to arise from closure of worm-like micelles due to the increasing water content (**Fig. 28**). Lateral aggregation and fusion of the worm-like micelles resulted also in primitive nano-sheets stabilized by thicker rims to partially release the

rim-cap energy. Rearrangement of the parallel-aligned FPOSS cylindrical cores generated hexagonally patterned nanosheets.

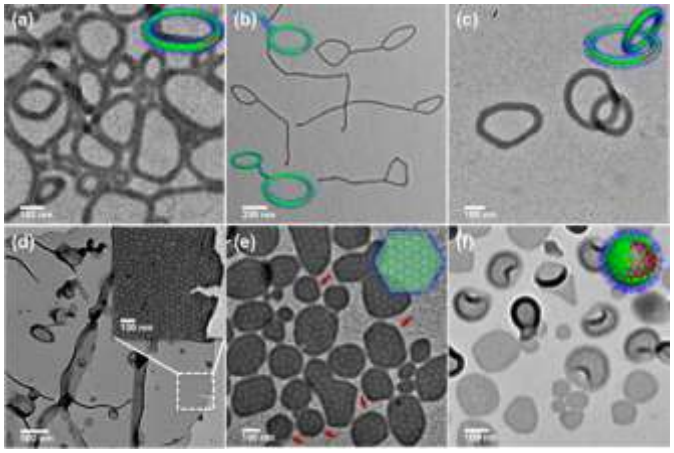

Fig. 28. TEM images of (a) toroids, (b) tadpoles and dumbbells, (c) interlocked toroids, (d, e) 2D nanosheets, and (f) laterally structured vesicles. FPOSS = red; PS = green; PEO = blue. Reproduced with the permission from ref. [191]. Copyright 2015 ACS.

7.6. Poly(Vinylidene fluoride)-based copolymers (PVDF)

In 2010, Gohy et al.[192] reported the self-assembly of the blend poly(VDF-*ter*-HFP-*ter*-TFMA) terpolymer and PS-*b*-P2VP-*b*-PEO triblock terpolymer (VDF = vinylidene fluoride, HFP = hexafluoropropene, TFMA = α-trifluoromethacrylic acid). The micellar solutions were obtained by first dissolving one of the blend partners in DMF, followed by the addition of the second blend partner as a powder. Formation of hydrogen-bonded complexes between TFMA and P2VP units was observed, leading to insoluble micelles of P2VP/poly(VDF-*ter*-HFP-*ter*-TFMA) terpolymer cores surrounded by a mixture of PS and PEO chains. Later, Asandei et al.[193] reported the self-assembly of PNaSS-*b*-PVDF-*b*-PNaSS triblock copolymers synthesized by deprotection of the neopentyl styrene sulfonate (NpSS) groups in PNpSS-*b*-PVDF-*b*-PNpSS triblock copolymers with NaN_3. Using methods 1 and 3, all the PNaSS-*b*-PVDF-*b*-PNaSS triblock copolymers provided colloidal stable nanoparticles in aqueous solution, even under the relatively high ionic strength of phosphate buffered saline (PBS) solutions (pH=7.4, 0.01 M phosphate buffer, 0.0027 M potassium chloride and 0.137 M sodium chloride). Ladmiral and co-workers reported the preparation and aqueous self-assembly of PVDF-*b*-PVA diblock copolymers obtained by RAFT polymerization followed by basic hydrolysis (PVA = poly(vinyl alcohol).[194] Using method 7, spherical nanoobjects with PVDF cores and PVA shells with diameters of about 147 nm were observed. Protocols of VDF RAFT dispersion polymerization in the presence of PVAc macro-CTAs were also published (PVAc = poly(vinyl acetate).[195] These PISA protocols afforded PVAc-*b*-PVDF branched micrometer-long crystalline morphologies resembling a desert rose. Although the self-assembly was triggered by the PVDF growing block, the morphologies of these structures are thought to be governed by the crystallization of PVDF. Crystallization Driven Self-Assembly (CDSA) approach was also employed by the same authors with amphiphilic PVDF-*b*-PDMAEMA block copolymers.[196] These BCPs were synthesized by CuAAC click chemistry of an azide-functionalized PVDF prepared by RAFT polymerization and three alkyne-functionalized PDMAEMAs prepared by ATRP. The three well-defined PVDF-*b*-PDMAEMA block copolymers were then self-assembled in water at three different pH. Mainly ill-defined spherical particles in the 20 to 500 nm size range were observed. However, micrometer-long cylindrical rigid micelles were obtained for PDMAEMA with DP =63 at pH 8.

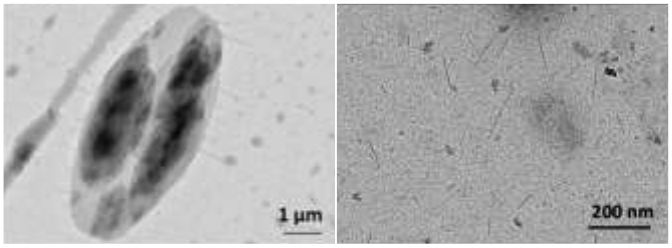

Fig. 29. Desert rose-like morphologies synthesized by PISA (PVAc-*b*-PVDF BCs, left) and cylindrical rigid micelles (PVDF-*b*-PDMAEMA BCs, right) reported by Ladmiral et al.[195,196]. Copyright 2017 RSC.

The same group also synthesized ABA triblock copolymers containing PVDF segments. Using a "one-pot" approach they prepared PVDF-*b*-PEG-*b*-PVDF and P(VDF-HFP)-*b*-PEG-*b*-P(VDF-HFP) via the efficient thia-Michael addition coupling of PVDF or P(VDF-HFP) prepared by RAFT, and a PEG diacrylate.[197,198] These symmetrical triblock copolymers led to various morphologies depending on the solvent mixtures and the self-assembly method. For example, the PVDF-*b*-PEG-*b*-PVDF in THF/ H_2O mixtures always formed vesicles regardless of the solvent ratios or self-assembly method. In contrast, when THF/ethanol mixtures (1:4 and 1:6) and method 2 were used, ovoidal shapes and crystalline shards were observed. These self-assemblies are believed to be governed by the high crystallinity of the PVDF block. Incorporation of HFP into the fluorinated blocks of the ABA triblock copolymer reduced the crystallinity and allowed easier access and control over the formation of uncommon crystalline structures.[198] In another study, Ladmiral et al. reported the synthesis and self-assembly of poly(*N*-isopropylacrylamide)-*b*-poly(vinylidene fluoride) and PNIPAM-*b*-PVDF amphiphilic block copolymers using RAFT polymerization. A PNIPAM macro-CTA was used to polymerize VDF in dimethyl carbonate (DMC). The as prepared diblock copolymers were self-assembled in various solvent mixtures using solvent CDSA method (method 2). Some of the outstanding morphologies observed were: crumpled spheres ($PNIPAM_{25}$-*b*-$PVDF_{35}$ and $PNIPAM_{35}$-*b*-$PVDF_{450}$ in DMF:water (1 : 4)), bilayer aggregates ($PNIPAM_{35}$-*b*-$PVDF_{450}$ in THF:water (1 : 4)), and 2D lenticular micelles ($PNIPAM_{25}$-*b*-$PVDF_{35}$ in acetone:water (1 : 4)).[199] Qian et al.[200] reported the self-assembly of commercially available PVDF-*b*-PS block copolymers. Micelle preparations were achieved via method 1 in different solvent mixture and using two different block copolymers ($PVDF_{180}$-*b*-PS_{125} and $PVDF_{180}$-*b*-PS_{1202}). Irregular spherical micelles were obtained except for $PVDF_{180}$-*b*-PS_{125} which led to worm-like micelles in DMF:1,4-dioxane (80:20).

7.7. Poly(ionic liquid)

Fluorinated poly(ionic liquid)s (PILs) have also attracted interest, either to promote morphology transitions when the fluorinated moieties were introduced as counter ions (e.g. the most used bis(trifluoromethylsulfonyl)imide($TFSI^-$)), or as a constituent of the backbone to induce self-organization. For instance, Vijayakrishna et al. reported a sudden yet fully reversible modification of PIL BCPs microstructures using anion exchange.[201] When bromide counter ion were exchanged with $TFSI^-$, reversible transition from micelles to vesicles was observed. Similar morphological transition (sphere to vesicle) was also observed with imidazolium poly(ionic liquid) when silver hexafluoroborate salt was employed.[202] This microstructure evolution trigered bycounter ion exchange was later confirmed by Isik et.al. They extended this concept to 4 different polyelectrolytes of different molar masses.[203] They demonstrated that the size of the nanoparticles could be tuned in the range of 100-600 nm depending on the chemical structure, the molar mass and the relative amount of $TFSI^-$ added vs the initial halide. He et al. reported the self-assembly of poly(acrylic acid*)-b*-poly(4-vinylbenzyl)-3-butyl imidazolium ($TFSI^-$) block copolymer into micelles, lamellae and cubosomes.[204] The morphologies were obtained in THF/H_2O mixtures using method 2 without removing the good solvent (THF) from the mixture. The cubosomes were particularly interesting considering their unique character in the context of BCP self-assembly.[205]

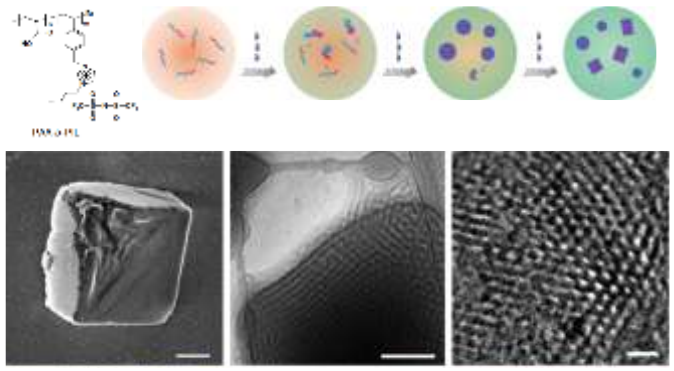

Figure 30. (top) BC structure and proposed self-assembly process of PAA-*b*-PIL in THF/H_2O mixture with the addition of water resulting in the formation of cubosomes. (bottom) SEM micrograph of the dried cubosomes after dialysis. (b) Cryo-TEM image of the [100] facet of a cuboid particle. (c) Enlarged surface image recorded in the central area of a cuboid particle from the [111] facet. Adapted with the permission from ref. [204]. Copyright Springer Nature 2016.

However, the formation of these nanostructures were only observed under very specific conditions with complex self-assembling pathway suggesting that ionic interactions could be one of the major governing parameters. Many other PIL BCPs microstructures were also reported with fluorinated counter ions such as $TFSI^-$, PF_6^-, BF_4^-, OTf^- ($CF_3SO_3^-$)etc. although the fluorinated contribution was not always the prevailing factor in the self-assembly.[206–208]

Lately, novel fluorinated-PIL featuring C_6F_{13} pendent groups as structuring agent able to promote self-assembly and ensure good thermal, mechanical and conductive properties were reported. In this study, the BCP synthesis was achieved via an elegant strategy involving a one-pot process using cobalt-mediated radical polymerization-induced self-assembly (CMR-PISA).[209]

Conclusion

Given the numerous potential applications of fluorinated copolymers, there is a constant growing interest in developing new methodologies to prepare them. Aside from coupling chemistries, the recent advances in reversible deactivation radical polymerization (RDRP) has opened new possibilities to prepare such copolymers. The aim of this review article was to gather a concise record of methods used to prepare fluorinated amphiphilic copolymers that led to self-assemblies in solution. Indeed, solution self-assembly is an attractive way to obtain colloidal stable nano-structures if it can be controlled and reproduced with high reliability. Given the wealth of properties that can brought by fluorinated polymer blocks (low Tg, crystallinity, O_2-philicity, hydrophobicity, oleophobicity, or ferroelectricity to name a few) fluorinated copolymers-based nano-objects should find applications in future nano-technologies.

Conflicts of interest

Authors declare no conflict of interest.

Acknowledgements

The authors thank Professor D. Taton for his precious advice.

Notes and references

1 S. C. Glotzer and M. J. Solomon, *Nat. Mater.*, 2007, **6**, 557–562.
2 J. Yan, M. Bloom, S. C. Bae, E. Luijten and S. Granick, *Nature*, 2012, **491**, 578–581.
3 A. H. Gröschel, A. Walther, T. I. Löbling, F. H. Schacher, H. Schmalz and A. H. E. Müller, *Nature*, 2013, **503**, 247–251.
4 L. Cademartiri and K. J. M. Bishop, *Nat. Mater.*, 2015, **14**, 2–9.
5 Z. Hua, J. R. Jones, M. Thomas, M. C. Arno, A. Souslov, T. R. Wilks and R. K. O'Reilly, *Nat. Commun.*, 2019, **10**, 1–8.
6 L. Zhang and A. Eisenberg, *Science*, 1995, **268**, 1728–1731.
7 L. Zhang and A. Eisenberg, *J. Am. Chem. Soc.*, 1996, **118**, 3168–3181.
8 D. E. Discher and A. Eisenberg, *Science*, 2002, **297**, 967–973.

9 U. Tritschler, S. Pearce, J. Gwyther, G. R. Whittell and I. Manners, *Macromolecules*, 2017, **50**, 3439–3463.

10 Y. Mai and A. Eisenberg, *Chem. Soc. Rev.*, 2012, **41**, 5969–5985.

11 J. Rodríguez-Hernández, F. Chécot, Y. Gnanou and S. Lecommandoux, *Prog. Polym. Sci.*, 2005, **30**, 691–724.

12 H. Qiu, Z. M. Hudson, M. A. Winnik and I. Manners, *Science*, 2015, **347**, 1329–1332.

13 J. Schmelz, F. H. Schacher and H. Schmalz, *Soft Matter*, 2013, **9**, 2101–2107.

14 N. Houbenov, R. Milani, M. Poutanen, J. Haataja, V. Dichiarante, J. Sainio, J. Ruokolainen, G. Resnati, P. Metrangolo and O. Ikkala, *Nat. Commun.*, 2014, **5**, 1–8.

15 L. Meazza, J. A. Foster, K. Fucke, P. Metrangolo, G. Resnati and J. W. Steed, *Nat. Chem.*, 2013, **5**, 42–47.

16 H. Cui, Z. Chen, S. Zhong, K. L. Wooley and D. J. Pochan, *Science*, 2007, **317**, 647–650.

17 Y. Yan, J. Huang and B. Z. Tang, *Chem. Commun.*, 2016, **52**, 11870–11884.

18 M. A. Hillmyer and T. P. Lodge, *J. Polym. Sci. Part Polym. Chem.*, 2002, **40**, 1–8.

19 C. K. Wong, X. Qiang, A. H. E. Müller and A. H. Gröschel, *Prog. Polym. Sci.*, 2020, 101211.

20 A. O. Moughton, M. A. Hillmyer and T. P. Lodge, *Macromolecules*, 2012, **45**, 2–19.

21 J. Huang, Y. Guo, S. Gu, G. Han, W. Duan, C. Gao and W. Zhang, *Polym. Chem.*, 2019, **10**, 3426–3435.

22 W. Yao, Y. Li and X. Huang, *Polymer*, 2014, **55**, 6197–6211.

23 J. Gardiner, *Aust. J. Chem.*, 2015, **68**, 13.

24 T. P. Lodge, A. Rasdal, Z. Li and M. A. Hillmyer, *J. Am. Chem. Soc.*, 2005, **127**, 17608–17609.

25 A. H. Gröschel, F. H. Schacher, H. Schmalz, O. V. Borisov, E. B. Zhulina, A. Walther and A. H. E. Müller, *Nat. Commun.*, 2012, **3**, 710.

26 Y. Zhao, F. Sakai, L. Su, Y. Liu, K. Wei, G. Chen and M. Jiang, *Adv. Mater.*, 2013, **25**, 5215–5256.

27 L. He, J. P. Hinestrosa, J. M. Pickel, S. Zhang, D. G. Bucknall, S. M. K. Ii, J. W. Mays and K. Hong, *J. Polym. Sci. Part Polym. Chem.*, 2011, **49**, 414–422.

28 H. Peng, K. J. Thurecht, I. Blakey, E. Taran and A. K. Whittaker, *Macromolecules*, 2012, **45**, 8681–8690.

29 K. Wang, H. Peng, K. J. Thurecht, S. Puttick and A. K. Whittaker, *Polym. Chem.*, 2016, **7**, 1059–1069.

30 G. Li, A. Xu, B. Geng, S. Yang, G. Wu and S. Zhang, *J. Fluor. Chem.*, 2014, **165**, 132–137.

31 P. I. R. Muraro, A. G. O. de Freitas, S. G. Trindade, F. C. Giacomelli, J.-J. Bonvent, V. Schmidt, F. P. dos Santos and C. Giacomelli, *J. Fluor. Chem.*, 2014, **168**, 251–259.

32 Q. Zhang and S. Zhu, *ACS Macro Lett.*, 2014, **3**, 743–746.

33 Y. Chen, Y. Zhang, Y. Wang, C. Sun and C. Zhang, *J. Appl. Polym. Sci.*, 2013, **127**, 1485–1492.

34 Y. Xu, W. Wang, Y. Wang, J. Zhu, D. Uhrig, X. Lu, J. K. Keum, J. W. Mays and K. Hong, *Polym. Chem.*, 2016, **7**, 680–688.

35 W. Du, A. M. Nyström, L. Zhang, K. T. Powell, Y. Li, C. Cheng, S. A. Wickline and K. L. Wooley, *Biomacromolecules*, 2008, **9**, 2826–2833.

36 K. Y. Mya, E. M. J. Lin, C. S. Gudipati, H. B. A. S. Gose and C. He, *J. Phys. Chem. B*, 2010, **114**, 9128–9134.

37 H. Liu, Y. Zhao, C. A. Dreiss and Y. Feng, *Soft Matter*, 2014, **10**, 6387–6391.

38 H. Liu, W. Wang, H. Yin and Y. Feng, *Langmuir*, 2015, **31**, 8756–8763.

39 H. Liu, Z. Guo, S. He, H. Yin and Y. Feng, *RSC Adv.*, 2016, **6**, 86728–86735.

40 S.-D. Xiong, L. Li, S.-L. Wu, Z.-S. Xu and P. K. Chu, *J. Polym. Sci. Part Polym. Chem.*, 2009, **47**, 4895–4907.

41 B. Jiang and H. Pang, *J. Polym. Sci. Part Polym. Chem.*, 2016, **54**, 992–1002.

42 J.-N. Marsat, M. Heydenreich, E. Kleinpeter, H. v. Berlepsch, C. Böttcher and A. Laschewsky, *Macromolecules*, 2011, **44**, 2092–2105.

43 Y.-N. Zhou, H. Cheng and Z.-H. Luo, *J. Polym. Sci. Part Polym. Chem.*, 2011, **49**, 3647–3657.

44 B. P. Koiry, A. Chakrabarty and N. K. Singha, *RSC Adv.*, 2015, **5**, 15461–15468.

45 B. P. Koiry, S. Ponnupandian, S. Choudhury and N. K. Singha, *J. Fluor. Chem.*, 2016, **189**, 51–58.

46 L. Yu, J.-J. Qiu, H. Cheng and Z.-H. Luo, *Mater. Chem. Phys.*, 2013, **138**, 780–786.

47 J. Chen, J.-J. Li and Z.-H. Luo, *J. Polym. Sci. Part Polym. Chem.*, 2013, **51**, 1107–1117.
48 M. V. de Paz Báñez, K. L. Robinson, V. Bütün and S. P. Armes, *Polymer*, 2001, **42**, 29–37.
49 J. Mao, P. Ni, Y. Mai and D. Yan, *Langmuir*, 2007, **23**, 5127–5134.
50 J. He, P. Ni and C. Liu, *J. Polym. Sci. Part Polym. Chem.*, 2008, **46**, 3029–3041.
51 Y. Hao, M. Zhang, J. Xu, C. Liu and P. Ni, *J. Macromol. Sci. Part A*, 2010, **47**, 941–951.
52 S. Li, J. He, M. Zhang, H. Wang and P. Ni, *Polym. Chem.*, 2016, **7**, 1773–1781.
53 X. Liu, Y. Ding, J. Liu, S. Lin and Q. Zhuang, *Eur. Polym. J.*, 2019, **116**, 342–351.
54 J. Liu, Y. Ding, X. Liu, S. Lin and Q. Zhuang, *Eur. Polym. J.*, 2019, **118**, 465–473.
55 S. Houvenagel, L. Moine, G. Picheth, C. Dejean, A. Brûlet, A. Chennevière, V. Faugeras, N. Huang, O. Couture and N. Tsapis, *Biomacromolecules*, 2018, **19**, 3244–3256.
56 K. Matsumoto, T. Ishizuka, T. Harada and H. Matsuoka, *Langmuir*, 2004, **20**, 7270–7282.
57 W. Wang, J. Zhang, C. Li, P. Huang, S. Gao, S. Han, A. Dong and D. Kong, *Colloids Surf. B Biointerfaces*, 2014, **115**, 302–309.
58 H. Hussain, K. Busse and J. Kressler, *Macromol. Chem. Phys.*, 2003, **204**, 936–946.
59 H. S. Hwang, H. J. Kim, Y. T. Jeong, Y.-S. Gal and K. T. Lim, *Macromolecules*, 2004, **37**, 9821–9825.
60 Y. Koda, T. Terashima and M. Sawamoto, *Macromolecules*, 2016, **49**, 4534–4543.
61 J. H. Ko, A. Bhattacharya, T. Terashima, M. Sawamoto and H. D. Maynard, *J. Polym. Sci. Part Polym. Chem.*, 2019, **57**, 352–359.
62 M. Matsumoto, M. Sawamoto and T. Terashima, *ACS Macro Lett.*, 2019, **8**, 320–325.
63 M. Y. Lee, S. H. Kim, J. T. Kim, S. W. Kim and K. T. Lim, *J. Nanosci. Nanotechnol.*, 2008, **8**, 4864–4868.
64 S. Xu and W. Liu, *J. Polym. Sci. Part B Polym. Phys.*, 2008, **46**, 1000–1006.
65 X. Dong, L. He, N. Wang, J.-Y. Liang, M.-J. Niu and X. Zhao, *J. Mater. Chem.*, 2012, **22**, 23078–23090.
66 Y. Zhang, L. Wang, Z. Zhang, Y. Zhang and X. Tuo, *J. Polym. Sci. Part Polym. Chem.*, 2013, **51**, 2161–2170.
67 A. Pan, S. Yang and L. He, *RSC Adv.*, 2015, **5**, 55048–55058.
68 X. Ma, L. He, S. Huang, Y. Wu, A. Pan and J. Liang, *Colloid Polym. Sci.*, 2020, **298**, 1559–1569.
69 T. Imae, H. Tabuchi, K. Funayama, A. Sato, T. Nakamura and N. Amaya, *Colloids Surf. Physicochem. Eng. Asp.*, 2000, **167**, 73–81.
70 K. Skrabania, A. Laschewsky, H. v. Berlepsch and C. Böttcher, *Langmuir*, 2009, **25**, 7594–7601.
71 H. v Berlepsch, C. Böttcher, K. Skrabania and A. Laschewsky, *Chem. Commun.*, 2009, 2290–2292.
72 K. Skrabania, H. v. Berlepsch, C. Böttcher and A. Laschewsky, *Macromolecules*, 2010, **43**, 271–281.
73 Y. Gao, X. Li, L. Hong and G. Liu, *Macromolecules*, 2012, **45**, 1321–1330.
74 X. Li, Y. Gao, X. Xing and G. Liu, *Macromolecules*, 2013, **46**, 7436–7442.
75 X. Li, B. Jin, Y. Gao, D. W. Hayward, M. A. Winnik, Y. Luo and I. Manners, *Angew. Chem. Int. Ed.*, 2016, **55**, 11392–11396.
76 B. Jin, K. Sano, S. Aya, Y. Ishida, N. Gianneschi, Y. Luo and X. Li, *Nat. Commun.*, 2019, **10**, 1–8.
77 X. Li, Y. Yang, G. Li and S. Lin, *Polym. Chem.*, 2014, **5**, 4553–4560.
78 G. Cavallo, P. Metrangolo, R. Milani, T. Pilati, A. Priimagi, G. Resnati and G. Terraneo, *Chem. Rev.*, 2016, **116**, 2478–2601.
79 A. Vanderkooy and M. S. Taylor, *J. Am. Chem. Soc.*, 2015, **137**, 5080–5086.
80 S. Banerjee, V. Ladmiral, A. Debuigne, C. Detrembleur, S. M. W. Rahaman, R. Poli and B. Ameduri, *Macromol. Rapid Commun.*, 2017, **38**, 1700203.
81 S. Banerjee, E. V. Bellan, F. Gayet, A. Debuigne, C. Detrembleur, R. Poli, B. Améduri and V. Ladmiral, *Polymers*, 2017, **9**, 702.
82 S. Banerjee, V. Ladmiral, C. Totée and B. Améduri, *Eur. Polym. J.*, 2018, **104**, 164–169.
83 P. G. Falireas, V. Ladmiral and B. Ameduri, *Polym. Chem.*, 2021, **12**, 277–290.
84 H. S. Hwang, J. Y. Heo, Y. T. Jeong, S.-H. Jin, D. Cho, T. Chang and K. T. Lim, *Polymer*, 2003, **44**, 5153–5158.
85 M. Niu, L. He, J. Liang, A. Pan and X. Zhao, *Prog. Org. Coat.*, 2014, **77**, 1603–1612.

86 C. Mugemana, B.-T. Chen, K. V. Bukhryakov and V. Rodionov, *Chem. Commun.*, 2014, **50**, 7862–7865.

87 B. Charleux, G. Delaittre, J. Rieger and F. D'Agosto, *Macromolecules*, 2012, **45**, 6753–6765.

88 S. L. Canning, G. N. Smith and S. P. Armes, *Macromolecules*, 2016, **49**, 1985–2001.

89 N. J. W. Penfold, J. Yeow, C. Boyer and S. P. Armes, *ACS Macro Lett.*, 2019, **8**, 1029–1054.

90 C. Liu, C.-Y. Hong and C.-Y. Pan, *Polym. Chem.*, 2020, **11**, 3673–3689.

91 F. D'Agosto, J. Rieger and M. Lansalot, *Angew. Chem. Int. Ed.*, 2020, **59**, 8368–8392.

92 A. B. Lowe, *Polymer*, 2016, **106**, 161–181.

93 X. Wang and Z. An, *Macromol. Rapid Commun.*, 2019, **40**, 1800325.

94 N. J. W. Penfold, J. Yeow, C. Boyer and S. P. Armes, *ACS Macro Lett.*, 2019, **8**, 1029–1054.

95 S. Li, G. Han and W. Zhang, *Polym. Chem.*, 2020, **11**, 4681–4692.

96 S. R. Mane, *New J. Chem.*, 2020, **44**, 6690–6698.

97 J. Rieger, *Macromol. Rapid Commun.*, 2015, **36**, 1458–1471.

98 M. Zong, K. J. Thurecht and S. M. Howdle, *Chem. Commun.*, 2008, **0**, 5942–5944.

99 A. Xu, Q. Lu, Z. Huo, J. Ma, B. Geng, U. Azhar, L. Zhang and S. Zhang, *RSC Adv.*, 2017, **7**, 51612–51620.

100 M. Semsarilar, E. R. Jones and S. P. Armes, *Polym. Chem.*, 2013, **5**, 195–203.

101 M. Semsarilar, V. Ladmiral, A. Blanazs and S. P. Armes, *Polym. Chem.*, 2014, **5**, 3466–3475.

102 B. Akpinar, L. A. Fielding, V. J. Cunningham, Y. Ning, O. O. Mykhaylyk, P. W. Fowler and S. P. Armes, *Macromolecules*, 2016, **49**, 5160–5171.

103 G. N. Smith, M. J. Derry, J. E. Hallett, J. R. Lovett, O. O. Mykhaylyk, T. J. Neal, S. Prévost and S. P. Armes, *Proc. R. Soc. Math. Phys. Eng. Sci.*, 2019, **475**, 20180763.

104 J. Jennings, E. J. Cornel, M. J. Derry, D. L. Beattie, M. J. Rymaruk, O. J. Deane, A. J. Ryan and S. P. Armes, *Angew. Chem. Int. Ed.*, 2020, **59**, 10848–10853.

105 L. Guo, Y. Jiang, T. Qiu, Y. Meng and X. Li, *Polymer*, 2014, **55**, 4601–4610.

106 W. Zhao, H. T. Ta, C. Zhang and A. K. Whittaker, *Biomacromolecules*, 2017, **18**, 1145–1156.

107 F. Ouhib, A. Dirani, A. Aqil, K. Glinel, B. Nysten, A. M. Jonas, C. Jerôme and C. Detrembleur, *Polym. Chem.*, 2016, **7**, 3998–4003.

108 X. Chen, J. Zhou and J. Ma, *RSC Adv.*, 2015, **5**, 97231–97238.

109 J. Zhou, X. Chen and J. Ma, *Prog. Org. Coat.*, 2016, **100**, 86–93.

110 J. Zhou, R. He and J. Ma, *Polymers*, 2016, **8**, 207.

111 J. Zhou, R. He and J. Ma, *Polymers*, 2016, **8**, 384.

112 M. Huo, M. Zeng, D. Li, L. Liu, Y. Wei and J. Yuan, *Macromolecules*, 2017, **50**, 8212–8220.

113 M. Huo, D. Li, G. Song, J. Zhang, D. Wu, Y. Wei and J. Yuan, *Macromol. Rapid Commun.*, 2018, **39**, 1700840.

114 M. Huo, Y. Zhang, M. Zeng, L. Liu, Y. Wei and J. Yuan, *Macromolecules*, 2017, **50**, 8192–8201.

115 S. Y. Khor, N. P. Truong, J. F. Quinn, M. R. Whittaker and T. P. Davis, *ACS Macro Lett.*, 2017, **6**, 1013–1019.

116 M. Huo, Z. Wan, M. Zeng, Y. Wei and J. Yuan, *Polym. Chem.*, 2018, **9**, 3944–3951.

117 M. Huo, M. Zeng, D. Wu, Y. Wei and J. Yuan, *Polym. Chem.*, 2018, **9**, 912–919.

118 B. Shi, H. Zhang, Y. Liu, J. Wang, P. Zhou, M. Cao and G. Wang, *Macromol. Rapid Commun.*, 2019, **n/a**, 1900547.

119 J.-M. Noy, A.-K. Friedrich, K. Batten, M. N. Bhebhe, N. Busatto, R. R. Batchelor, A. Kristanti, Y. Pei and P. J. Roth, *Macromolecules*, 2017, **50**, 7028–7040.

120 G. Delaittre and L. Barner, *Polym. Chem.*, 2018, **9**, 2679–2684.

121 J.-M. Noy, Y. Li, W. Smolan and P. J. Roth, *Macromolecules*, 2019, **52**, 3083–3091.

122 D. Le, D. Keller and G. Delaittre, *Macromol. Rapid Commun.*, 2019, **40**, 1800551.

123 Y. Pei, J.-M. Noy, P. J. Roth and A. B. Lowe, *Polym. Chem.*, 2015, **6**, 1928–1931.

124 Y. Pei, J.-M. Noy, P. J. Roth and A. B. Lowe, *J. Polym. Sci. Part Polym. Chem.*, 2015, **53**, 2326–2335.

125 N. Busatto, V. Stolojan, M. Shaw, J. L. Keddie and P. J. Roth, *Macromol. Rapid Commun.*, 2019, **40**, 1800346.
126 N. Busatto, J. L. Keddie and P. J. Roth, *Polym. Chem.*, 2019, **11**, 704–711.
127 S. Kubowicz, J.-F. Baussard, J.-F. Lutz, A. F. Thünemann, H. von Berlepsch and A. Laschewsky, *Angew. Chem. Int. Ed.*, 2005, **44**, 5262–5265.
128 H. Cui, Z. Chen, S. Zhong, K. L. Wooley and D. J. Pochan, *Science*, 2007, **317**, 647–650.
129 C. S. Gudipati, M. B. H. Tan, H. Hussain, Y. Liu, C. He and T. P. Davis, *Macromol. Rapid Commun.*, 2008, **29**, 1902–1907.
130 B. H. Tan, H. Hussain, Y. Liu, C. B. He and T. P. Davis, *Langmuir*, 2010, **26**, 2361–2368.
131 H. Hussain, B. H. Tan, K. Y. Mya, Y. Liu, C. B. He and T. P. Davis, *J. Polym. Sci. Part Polym. Chem.*, 2010, **48**, 152–163.
132 W. Du, Y. Li, A. M. Nyström, C. Cheng and K. L. Wooley, *J. Polym. Sci. Part Polym. Chem.*, 2010, **48**, 3487–3496.
133 C. Song, D. Ao, X. Wang, J. Zhang and Y. Tan, *Colloid Polym. Sci.*, 2013, **291**, 2815–2823.
134 F. Lv, Z. An and P. Wu, *Nat. Commun.*, 2019, **10**, 1–7.
135 F. Lv, Z. An and P. Wu, *Macromolecules*, 2020, **53**, 367–373.
136 Z. Li, E. Kesselman, Y. Talmon, M. A. Hillmyer and T. P. Lodge, *Science*, 2004, **306**, 98–101.
137 Z. Li, M. A. Hillmyer and T. P. Lodge, *Macromolecules*, 2004, **37**, 8933–8940.
138 Z. Li, M. A. Hillmyer and T. P. Lodge, *Langmuir*, 2006, **22**, 9409–9417.
139 A. N. Semenov, I. A. Nyrkova and A. R. Khokhlov, *Macromolecules*, 1995, **28**, 7491–7500.
140 Z. Li, M. A. Hillmyer and T. P. Lodge, *Nano Lett.*, 2006, **6**, 1245–1249.
141 C. Liu, M. A. Hillmyer and T. P. Lodge, *Langmuir*, 2008, **24**, 12001–12009.
142 Z. Li, M. A. Hillmyer and T. P. Lodge, *Macromolecules*, 2006, **39**, 765–771.
143 T. P. Lodge, A. Rasdal, Z. Li and M. A. Hillmyer, *J. Am. Chem. Soc.*, 2005, **127**, 17608–17609.
144 A. O. Moughton, T. Sagawa, L. Yin, T. P. Lodge and M. A. Hillmyer, *ACS Omega*, 2016, **1**, 1027–1033.
145 A. F. Thünemann, S. Kubowicz, H. von Berlepsch and H. Möhwald, *Langmuir*, 2006, **22**, 2506–2510.
146 Z. Li, M. A. Hillmyer and T. P. Lodge, *Langmuir*, 2006, **22**, 9409–9417.
147 R. R. Taribagil, M. A. Hillmyer and T. P. Lodge, *Macromolecules*, 2010, **43**, 5396–5404.
148 R. R. Taribagil, M. A. Hillmyer and T. P. Lodge, *Macromolecules*, 2009, **42**, 1796–1800.
149 Z. Zhang, X. Hao, P. A. Gurr, A. Blencowe, T. C. Hughes and G. G. Qiao, *Aust. J. Chem.*, 2012, **65**, 1186–1190.
150 G. Lopez, M. Guerre, J. Schmidt, Y. Talmon, V. Ladmiral, J.-P. Habas and B. Améduri, *Polym. Chem.*, 2015, **7**, 402–409.
151 W. F. Edmonds, M. A. Hillmyer and T. P. Lodge, *Macromolecules*, 2007, **40**, 4917–4923.
152 T. S. Kaminski, O. Scheler and P. Garstecki, *Lab. Chip*, 2016, **16**, 2168–2187.
153 I. Platzman, J.-W. Janiesch and J. P. Spatz, *J. Am. Chem. Soc.*, 2013, **135**, 3339–3342.
154 T. Gao, X. Gu, S. Guo and G. Wang, *Polymer*, 2020, **205**, 122732.
155 D. A. Babb, B. R. Ezzell, K. S. Clement, W. F. Richey and A. P. Kennedy, *J. Polym. Sci. Part Polym. Chem.*, 1993, **31**, 3465–3477.
156 Y. Li, S. Zhang, L. Tong, Q. Li, W. Li, G. Lu, H. Liu and X. Huang, *J. Fluor. Chem.*, 2009, **130**, 354–360.
157 D. W. Smith, S. T. Iacono and S. S. Iyer, *Handbook of Fluoropolymer Science and Technology*, John Wiley&Sons, Inc.: Hoboken., 2014.
158 L. Tong, Z. Shen, D. Yang, S. Chen, Y. Li, J. Hu, G. Lu and X. Huang, *Polymer*, 2009, **50**, 2341–2348.
159 D. Yang, L. Tong, Y. Li, J. Hu, S. Zhang and X. Huang, *Polymer*, 2010, **51**, 1752–1760.
160 Y. Li, S. Zhang, H. Liu, Q. Li, W. Li and X. Huang, *J. Polym. Sci. Part Polym. Chem.*, 2010, **48**, 5419–5429.
161 W. Yao, Y. Li, S. Zhang, H. Liu and X. Huang, *J. Polym. Sci. Part Polym. Chem.*, 2011, **49**, 4433–4440.
162 W. Yao, Y. Li, C. Feng, G. Lu and X. Huang, *Polym. Chem.*, 2014, **5**, 6334–6343.

163 W. Yao, Y. Li, C. Feng, G. Lu and X. Huang, *RSC Adv.*, 2014, **4**, 52105–52116.
164 C. Feng, C. Zhu, W. Yao, G. Lu, Y. Li, X. Lv, M. Jia and X. Huang, *Polym. Chem.*, 2015, **6**, 7881–7892.
165 G. Lu, H. Liu, H. Gao, C. Feng, Y. Li and X. Huang, *RSC Adv.*, 2015, **5**, 39668–39676.
166 H. Liu, S. Zhang, C. Feng, Y. Li, G. Lu and X. Huang, *Polym. Chem.*, 2015, **6**, 4309–4318.
167 R. Hoogenboom, *Angew. Chem. Int. Ed.*, 2009, **48**, 7978–7994.
168 C. Weber, R. Hoogenboom and U. S. Schubert, *Prog. Polym. Sci.*, 2012, **37**, 686–714.
169 F. Wiesbrock, R. Hoogenboom, M. A. M. Leenen, M. A. R. Meier and U. S. Schubert, *Macromolecules*, 2005, **38**, 5025–5034.
170 F. Wiesbrock, R. Hoogenboom and U. S. Schubert, *Macromol. Rapid Commun.*, 2004, **25**, 1739–1764.
171 T. Kagiya, S. Narisawa, T. Maeda and K. Fukui, *J. Polym. Sci. [B]*, 1966, **4**, 441–445.
172 W. Seeliger, E. Aufderhaar, W. Diepers, R. Feinauer, R. Nehring, W. Thier and H. Hellmann, *Angew. Chem. Int. Ed. Engl.*, 1966, **5**, 875–888.
173 D. A. Tomalia and D. P. Sheetz, *J. Polym. Sci. [A1]*, 1966, **4**, 2253–2265.
174 T. G. Bassiri, A. Levy and M. Litt, *J. Polym. Sci. [B]*, 1967, **5**, 871–879.
175 R. Ivanova, T. Komenda, T. B. Bonné, K. Lüdtke, K. Mortensen, P. K. Pranzas, R. Jordan and C. M. Papadakis, *Macromol. Chem. Phys.*, 2008, **209**, 2248–2258.
176 M. Lobert, R. Hoogenboom, C.-A. Fustin, J.-F. Gohy and U. S. Schubert, *J. Polym. Sci. Part Polym. Chem.*, 2008, **46**, 5859–5868.
177 K. Kempe, R. Hoogenboom, S. Hoeppener, C.-A. Fustin, J.-F. Gohy and U. S. Schubert, *Chem. Commun.*, 2010, **46**, 6455–6457.
178 U. Mansfeld, S. Hoeppener, K. Kempe, J.-M. Schumers, J.-F. Gohy and U. S. Schubert, *Soft Matter*, 2013, **9**, 5966–5974.
179 J. M. Bak, K.-B. Kim, J.-E. Lee, Y. Park, S. S. Yoon, H. M. Jeong and H. Lee, *Polym. Chem.*, 2013, **4**, 2219–2223.
180 J. M. Bak and H. Lee, *J. Polym. Sci. Part Polym. Chem.*, 2013, **51**, 1976–1982.
181 X. Jiang, F. Chun, G. Lu and H. Xiaoyu, *Polym. Chem.*, 2017, **8**, 1163–1176.
182 K. Matsumoto, M. Kubota, H. Matsuoka and H. Yamaoka, *Macromolecules*, 1999, **32**, 7122–7127.
183 K. Matsumoto, H. Mazaki, R. Nishimura, H. Matsuoka and H. Yamaoka, *Macromolecules*, 2000, **33**, 8295–8300.
184 K. Matsumoto, H. Mazaki and H. Matsuoka, *Macromolecules*, 2004, **37**, 2256–2267.
185 B. Fang, A. Walther, A. Wolf, Y. Xu, J. Yuan and A. H. E. Müller, *Angew. Chem. Int. Ed.*, 2009, **48**, 2877–2880.
186 X. Wang, K. Hong, D. Baskaran, M. Goswami, B. Sumpter and J. Mays, *Soft Matter*, 2011, **7**, 7960–7964.
187 S. Suárez-Suárez, G. A. Carriedo and A. Presa Soto, *Chem. – Eur. J.*, 2016, **22**, 4483–4491.
188 D. Presa-Soto, G. A. Carriedo, R. de la Campa and A. Presa Soto, *Angew. Chem. Int. Ed.*, 2016, **55**, 10102–10107.
189 D. R. Ratnaweera, U. M. Shrestha, N. Osti, C.-M. Kuo, S. Clarson, K. Littrell and D. Perahia, *Soft Matter*, 2012, **8**, 2176–2184.
190 Z. M. Hudson, J. Qian, C. E. Boott, M. A. Winnik and I. Manners, *ACS Macro Lett.*, 2015, **4**, 187–191.
191 B. Ni, M. Huang, Z. Chen, Y. Chen, C.-H. Hsu, Y. Li, D. Pochan, W.-B. Zhang, S. Z. D. Cheng and X.-H. Dong, *J. Am. Chem. Soc.*, 2015, **137**, 1392–1395.
192 J.-F. Gohy, N. Lefèvre, C. D'Haese, S. Hoeppener, U. S. Schubert, G. Kostov and B. Améduri, *Polym. Chem.*, 2011, **2**, 328–332.
193 P. Černoch, Z. Černochová, S. Petrova, D. Kaňková, J.-S. Kim, V. Vasu and A. D. Asandei, *RSC Adv.*, 2016, **6**, 55374–55381.
194 M. Guerre, J. Schmidt, Y. Talmon, B. Améduri and V. Ladmiral, *Polym. Chem.*, 2017, **8**, 1125–1128.
195 M. Guerre, M. Semsarilar, F. Godiard, B. Améduri and V. Ladmiral, *Polym. Chem.*, 2017, **8**, 1477–1487.
196 M. Guerre, M. Semsarilar, C. Totée, G. Silly, B. Améduri and V. Ladmiral, *Polym. Chem.*, 2017, **8**, 5203–5211.
197 E. Folgado, M. Guerre, A. D. Costa, A. Ferri, A. Addad, V. Ladmiral and M. Semsarilar, *Polym. Chem.*, 2020, **11**, 401–410.

198 E. Folgado, M. Mayor, V. Ladmiral and M. Semsarilar, *Molecules*, 2020, **25**, 4033.
199 E. Folgado, M. Mayor, D. Cot, M. Ramonda, F. Godiard, V. Ladmiral and M. Semsarilar, *Polym. Chem.*, , DOI:10.1039/D0PY01193B.
200 Y. Wu, L. Chen, X. Sun, J. Xu, G. Gu and J. Qian, *J. Saudi Chem. Soc.*, 2017, **21**, 713–719.
201 K. Vijayakrishna, D. Mecerreyes, Y. Gnanou and D. Taton, *Macromolecules*, 2009, **42**, 5167–5174.
202 J. Guo, Y. Zhou, L. Qiu, C. Yuan and F. Yan, *Polym. Chem.*, 2013, **4**, 4004–4009.
203 M. Isik, A. M. Fernandes, K. Vijayakrishna, M. Paulis and D. Mecerreyes, *Polym. Chem.*, 2016, **7**, 1668–1674.
204 H. He, K. Rahimi, M. Zhong, A. Mourran, D. R. Luebke, H. B. Nulwala, M. Möller and K. Matyjaszewski, *Nat. Commun.*, 2017, **8**, 14057.
205 A. H. Gröschel and A. Walther, *Angew. Chem. Int. Ed.*, 2017, **56**, 10992–10994.
206 V. Baddam, R. Missonen, S. Hietala and H. Tenhu, *Macromolecules*, 2019, **52**, 6514–6522.
207 H. Luo, Q. Tang, J. Zhong, Z. Lei, J. Zhou and Z. Tong, *Macromol. Chem. Phys.*, 2019, **220**, 1800508.
208 Y. Yang, J. Zheng, S. Man, X. Sun and Z. An, *Polym. Chem.*, 2018, **9**, 824–827.
209 D. Cordella, F. Ouhib, A. Aqil, T. Defize, C. Jérôme, A. Serghei, E. Drockenmuller, K. Aissou, D. Taton and C. Detrembleur, *ACS Macro Lett.*, 2017, **6**, 121–126.